

# MAVRL: Learning Reward Functions from Multiple Feedback Types with Amortized Variational Inference

Raphaël Baur<sup>1,2</sup> Yannick Metz<sup>2</sup> Maria Gkoultz<sup>2</sup> Mennatallah El-Assady<sup>1,2</sup>  
 Giorgia Ramponi<sup>1,3</sup> Thomas Kleine Buening<sup>1,2</sup>

<sup>1</sup> ETH AI Center, ETH Zurich  
<sup>2</sup> Department of Computer Science, ETH Zurich  
<sup>3</sup> Department of Informatics, University of Zurich

raphael.baur@ai.ethz.ch

## Abstract

Reward learning typically relies on a single feedback type or combines multiple feedback types using manually weighted loss terms. Currently, it remains unclear how to jointly learn reward functions from heterogeneous feedback types such as demonstrations, comparisons, ratings, and stops that provide qualitatively different signals. We address this challenge by formulating reward learning from multiple feedback types as Bayesian inference over a shared latent reward function, where each feedback type contributes information through an explicit likelihood. We introduce a scalable amortized variational inference approach that learns a shared reward encoder and feedback-specific likelihood decoders and is trained by optimizing a single evidence lower bound. Our approach avoids reducing feedback to a common intermediate representation and eliminates the need for manual loss balancing. Across discrete and continuous-control benchmarks, we show that jointly inferred reward posteriors outperform single-type baselines, exploit complementary information across feedback types, and yield policies that are more robust to environment perturbations. The inferred reward uncertainty further provides interpretable signals for analyzing model confidence and consistency across feedback types.

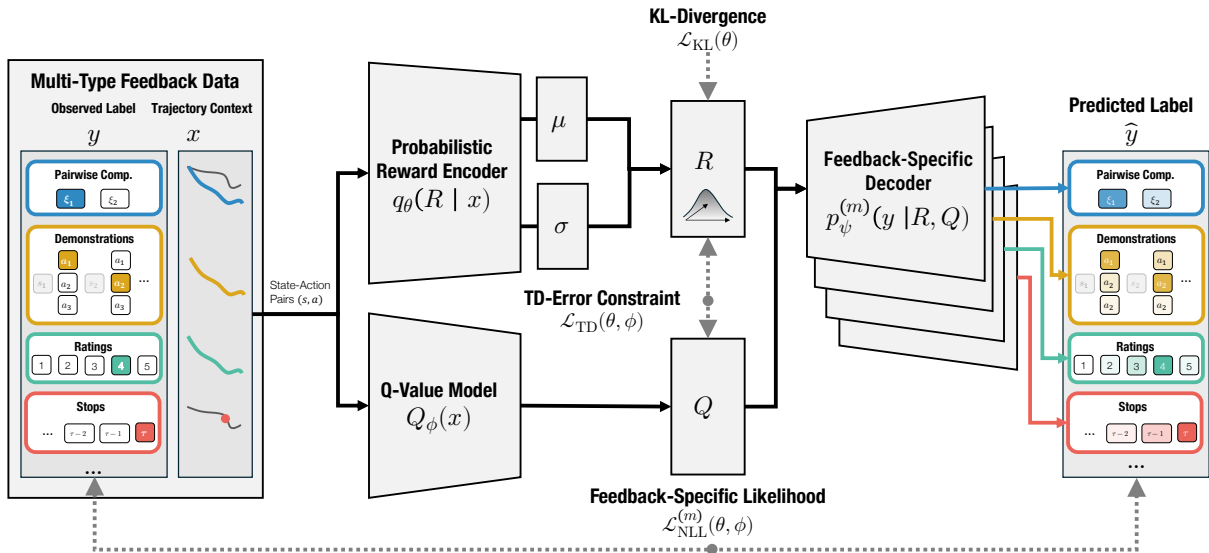


Figure 1: Overview of MAVRL. A shared variational reward encoder predicts reward samples from state-action pairs for each feedback modality. A jointly optimized Q-value model estimates optimal values for the same transitions. Both reward samples and Q-values are passed to modality-specific decoders, which maximize their respective likelihoods. A KL-divergence regularizer enforces consistency with a standard normal prior, while a TD-error constraint aligns reward and Q-value estimates through one-step Bellman differences. MAVRL is naturally extensible since incorporating additional feedback types only requires adding a corresponding likelihood decoder.

# 1 Introduction

Designing reward functions that faithfully capture desired behavior is notoriously difficult. Even in well-specified environments, subtle preferences, safety considerations, and trade-offs are hard to encode by hand, and small misspecifications can lead to unintended or unsafe behavior (Abouelazm et al., 2024; Amodei et al., 2016; Gershman and Niv, 2015; Hendrycks et al., 2021; Knox et al., 2023). This challenge has motivated a broad line of work on reward learning, where reward functions are inferred from human feedback rather than specified explicitly. Such approaches are appealing because they allow domain experts to communicate intent through judgments or interventions that are often easier to provide than a complete formal specification.

Human feedback about behavior, however, comes in many forms. Previous work has studied learning from demonstrations (Chan and van der Schaar, 2021; Ng et al., 2000), comparisons or preferences (Christiano et al., 2017; Wirth et al., 2016), scalar ratings (Knox and Stone, 2009), rankings (Brown et al., 2019; Myers et al., 2021), and interventions such as corrections or emergency stops (Ghosal et al., 2023; Hadfield-Menell et al., 2017; Losey et al., 2022), among others. Each feedback type provides only partial information about the underlying reward function: demonstrations offer sparse coverage of the state-action space and constrain rewards only along the expert behaviors; comparisons provide relative information about returns without fully specifying trade-offs beyond the compared alternatives; ratings only provide ordinal information about trajectories while discarding preference strength; and stops typically indicate unacceptable behavior without specifying what would have been optimal instead. As a result, relying on any single feedback type can leave aspects of the reward undetermined.

These limitations highlight the need for learning from multiple feedback types, as different modalities can provide complementary information that resolves ambiguities left by any single source. Moreover, feedback types differ in availability, cost, and informativeness, making it important to understand how they relate to one another, how much information they provide, where they overlap, and when they conflict.

Despite their complementary potential, learning reward functions jointly from heterogeneous feedback types remains challenging. Existing approaches either train separate reward models for each feedback type and combine them post hoc (Ibarz et al., 2018; Macuglia et al., 2025; Metz et al., 2025), or focus on a narrow subset of modalities, typically demonstrations and comparisons (Biyik et al., 2022). Both strategies introduce significant challenges: post hoc aggregation raises questions about how to reconcile reward scales and uncertainties across feedback types, while collapsing diverse feedback into a single intermediate representation (such as preferences) can obscure modality-specific information and is not applicable to all forms of feedback. As a result, despite their complementary potential, jointly learning reward functions from multiple types of feedback remains difficult in practice.

A more principled perspective is to view each feedback type as a probabilistic observation of a shared latent reward function. Under this formulation, learning from multiple feedback types naturally corresponds to Bayesian inference, where each feedback modality contributes information through its likelihood. Several frameworks formalize human feedback in this manner, for example, by modeling feedback as reward-rational choices from (possibly implicit) choice sets (Jeon et al., 2020). This likelihood-based formulation provides a conceptually unified treatment of heterogeneous feedback and makes explicit how different feedback types relate to the same underlying reward. However, exact Bayesian inference in this setting is generally intractable due to the need to marginalize over both feedback realizations and reward functions.

To address these challenges, we introduce a scalable amortized variational inference approach for learning reward functions from multiple feedback types. Building on prior work on scalable Bayesian inverse reinforcement learning (Chan and van der Schaar, 2021), our method learns a shared variational reward representation together with feedback-specific likelihood models and is trained by optimizing a single evidence lower bound.

**Contributions** Concretely, our contributions are as follows:

- We introduce a unified Bayesian formulation for learning reward functions from multiple feedback types, where each feedback modality contributes information through an explicit likelihood and no manual loss balancing is required (Section 4).
- We propose a scalable amortized variational inference algorithm that jointly learns a shared reward representation together with feedback-specific likelihood models (Section 5).
- We empirically demonstrate that jointly learning from multiple feedback types exploits complementary information, improves reward recovery and policy robustness, and yields interpretable reward uncertainty across a range of reinforcement learning benchmarks (Section 6).

## 2 Related Work

**Reward Learning.** Reward learning seeks to infer reward functions from human feedback when explicit reward specification is impractical (Abbeel and Ng, 2004; Christiano et al., 2017; Ng et al., 2000). Early work focused on inverse reinforcement learning (IRL) from demonstrations, assuming expert trajectories arise from (approximately) optimal behavior under an unknown reward (Abbeel and Ng, 2004; Ng et al., 2000). More recently, preference-based reinforcement learning has gained prominence, particularly through applications in language modeling, where humans compare agent trajectory segments and reward models are trained using the Bradley-Terry model or related probabilistic choice formulations (Christiano et al., 2017; Ouyang et al., 2022).

Beyond demonstrations and preferences, a variety of other feedback types have been explored, including corrections (Bajcsy et al., 2017; Losey et al., 2022), rankings (Brown et al., 2020; Myers et al., 2021), and emergency stops (Hadfield-Menell et al., 2017). Each feedback paradigm introduces its own modeling assumptions and loss functions, and is typically studied in isolation. A unifying perspective was proposed by Jeon et al. (2020), who showed that many feedback types can be interpreted as reward-rational choices from (possibly implicit) choice sets. While this framework provides a common probabilistic interpretation of feedback, it does not by itself yield a scalable method for jointly learning from heterogeneous feedback sources.

**Approximate Inference for Bayesian IRL.** Closely related to our work is the literature on scalable Bayesian IRL. Bayesian IRL poses reward learning from demonstrations as posterior inference, but early methods relied on MCMC or other sampling-based inference methods, limiting their applicability to small tasks (Ramachandran and Amir, 2007; Rothkopf and Dimitrakakis, 2011).

To address this, Chan and van der Schaar (2021) proposed AVRIL, which applies amortized variational inference to Bayesian IRL by jointly learning a variational reward encoder and a demonstration likelihood decoder. This formulation enables efficient posterior inference without repeatedly solving a reinforcement learning problem in an inner loop and has been shown to scale to high-dimensional control as well as transformer-based reward models in language modeling (Cai et al., 2025).

Other recent work has applied variational inference to preference learning to capture user-specific reward variation, but with a different objective than learning a shared reward function from multi-type feedback (Poddar et al., 2024). We build directly on the AVRIL framework by replacing its single demonstration likelihood with a set of feedback-specific likelihood models, while maintaining a single shared variational posterior over reward functions. This enables joint amortized inference from several feedback types without collapsing them into a common surrogate objective.

**Multi-Type Feedback.** Compared to single-type reward learning, relatively little work has studied learning from multiple types of human feedback. Most existing efforts focus on demonstrations and preferences, and use demonstrations primarily as an initialization step before applying preference-based learning to further refine the policy and reward estimates (Biyik et al., 2022; Ibarz et al., 2018; Macuglia et al., 2025; Palan et al., 2019).

A small number of approaches attempt to incorporate more than two feedback types within a single learning procedure. Mehta and Losey (2024) integrate demonstrations, corrections, and preferences using the reward-rational choice framework in a robotics setting, but ultimately combines modalities through additive loss terms whose relative influence is fixed by design choices (e.g., sampling rates).

Recent benchmark suites and evaluation platforms emphasize the practical relevance of heterogeneous feedback (Metz et al., 2023; Yuan et al., 2024), and existing large-scale studies evaluate combinations of feedback types using ensemble-style approaches (Metz et al., 2025). However, these approaches do not perform joint inference over a single reward function and instead rely on heuristics to reconcile different reward scales and uncertainties across feedback types.

In contrast, our approach performs joint Bayesian inference over a shared reward function from multi-type feedback by integrating feedback-specific likelihoods within a single variational objective.

## 3 Preliminaries

We consider Markov Decision Processes (MDPs)  $\mathcal{M} = (\mathcal{S}, \mathcal{A}, T, R^*, \gamma)$  with state space  $\mathcal{S}$ , action space  $\mathcal{A}$ , transition dynamics  $T(s' | s, a)$ , ground-truth reward function  $R^* : \mathcal{S} \times \mathcal{A} \rightarrow \mathbb{R}$ , and discount factor  $\gamma \in [0, 1)$ . Both  $\mathcal{S}$  and  $\mathcal{A}$  may be discrete or continuous, and we do not assume access to the transition dynamics. Moreover, the reward function  $R^*$  is assumed to be unobserved.

The agent interacts with the MDP via a (possibly stochastic) stationary policy  $\pi(a|s)$ , which induces a distribution over trajectories  $\xi = (s_0, a_0, s_1, a_1, \dots)$  in the MDP. We denote by  $\Pi$  the space of all stationary policies and with  $\Xi$  the space of all trajectories.<sup>1</sup> Given a reward function  $R$ , the return of a trajectory  $\xi$  is  $R(\xi) = \sum_{t=0}^{\infty} \gamma^t R(s_t, a_t)$ , and the expected return of a policy  $\pi$  is  $R(\pi) = \mathbb{E}_{\xi \sim \pi}[R(\xi)]$ . For a given reward function  $R$ , we let  $Q_R^*(s, a) = \sup_{\pi \in \Pi} \mathbb{E}_{\xi \sim \pi}[R(\xi) \mid s_0 = s, a_0 = a]$  denote the optimal action-value function.

**Bayesian Learning from Multi-Type Feedback.** Given a set of multi-type human feedback  $\mathcal{D}$ , we are interested in learning a reward function. Concretely, we consider  $\mathcal{D} = \{\mathcal{D}^{(m)}\}_{m=1}^M$ , where  $\mathcal{D}^{(m)}$  corresponds to feedback of type  $m$  (e.g., preferences).

Taking the Bayesian perspective, our goal is to infer a posterior distribution over the reward function given this data. Following this, we treat the reward function  $R$  as a latent variable and consider

$$p(R \mid \mathcal{D}) = \frac{p(\mathcal{D} \mid R)p(R)}{\int p(\mathcal{D} \mid R')p(R') \, dR'}, \quad (1)$$

where  $p(R)$  is a prior over reward functions and  $p(\mathcal{D} \mid R)$  is the likelihood of observing the multi-type feedback  $\mathcal{D}$  under  $R$ . Crucially, the likelihood of observed feedback conditional on  $R$  factorizes in a useful manner. As the observations are conditionally independent given the reward function, we can express the joint likelihood as  $p(\mathcal{D} \mid R) = \prod_m p(\mathcal{D}^{(m)} \mid R)$ . Hence, the multi-type feedback posterior satisfies  $p(R \mid \mathcal{D}) \propto \prod_m p(\mathcal{D}^{(m)} \mid R)p(R)$ .

**Amortized Variational Inference.** Although elegant, equation (1) is generally doubly intractable: first due to the integration over feedback choices in the likelihood term, and second due to the integration over all possible reward functions in the denominator. *Variational inference* (VI) addresses this intractability by approximating the posterior with a simpler *variational* distribution  $q_\theta(R) \approx p(R \mid \mathcal{D})$ . Its parameters  $\theta$  can then be learned by maximizing the evidence lower bound (ELBO):

$$\mathbb{E}_{R \sim q_\theta(\cdot)} [\log p(\mathcal{D} \mid R)] - D_{\text{KL}}(q_\theta(R) \parallel p(R)). \quad (2)$$

The first term maximizes the expected data likelihood, while the second imposes a soft regularization that penalizes deviations of the variational distribution  $q_\theta(R)$  from the assumed prior  $p(R)$ .

The *Variational Autoencoder* (VAE) framework (Kingma and Welling, 2014) made variational inference broadly applicable and scalable by representing the variational distribution  $q_\theta(z \mid x)$  as a neural network *encoder* that maps observations  $x$  to latent variables  $z$ , thereby *amortizing* posterior inference across data points. In addition, VAEs jointly learn a likelihood model  $p_\phi(y \mid z)$ , the *decoder*, which reconstructs the observed response  $y$  from the latent representation  $z$ .<sup>2</sup> This is enabled through the *reparameterization trick*, which expresses sampling as a deterministic transformation  $z = g_\theta(\epsilon, x)$  with  $\epsilon \sim p(\cdot)$ , allowing gradients to flow through the encoder.

## 4 Feedback-Specific Likelihood Models

We define probabilistic likelihood models for each feedback type, which together induce the joint data likelihood  $p(\mathcal{D} \mid R)$  in the Bayesian reward learning objective (Eq. 1) and therefore determine the variational objective optimized by our algorithm. In this paper, we focus on *preferences* (pairwise comparisons), *demonstrations*, *ratings*, and *stops*, but the proposed framework and algorithm apply to any feedback type for which a probabilistic likelihood can be specified. Importantly, our method is agnostic to the particular choice of likelihood model and does not rely on shared intermediate representations or manual loss balancing across feedback types.

**Preferences (PDRS).** We here employ the commonly used Bradley-Terry model under which a trajectory  $\xi_1$  is preferred over  $\xi_2$  under the reward function  $R$  with probability:

$$p(\xi_1 \succ \xi_2 \mid R) = \frac{\exp(\beta R(\xi_1))}{\exp(\beta R(\xi_1)) + \exp(\beta R(\xi_2))}.$$

This formulation naturally extends to comparisons between trajectory segments, as in Christiano et al. (2017). The inverse temperature parameter  $\beta$  controls the stochasticity of the preference judgments.

<sup>1</sup>All definitions and results extend straightforwardly to finite-horizon MDPs by replacing the infinite discounted sum with a finite-horizon return. We adopt the infinite-horizon discounted formulation for notational convenience.

<sup>2</sup>Typically, in VAEs, the objective is to learn meaningful latent representations  $z$  through a reconstruction task, where  $x = y$ .

**Demonsations (PDRS).** Expert demonstrations represent another commonly used form of feedback. [Ramachandran and Amir \(2007\)](#) and subsequent work, e.g., [Chan and van der Schaar \(2021\)](#); [Rothkopf and Dimitrakakis \(2011\)](#), model expert demonstrations through a Boltzmann-rational policy  $\pi(a | s, R) \propto \exp(\beta Q_R^*(s, a))$ . We follow their modeling so that the likelihood of an expert trajectory  $\xi$  under the reward function  $R$  is given by

$$p(\xi | R) = \prod_{(s,a) \in \xi} \frac{\exp(\beta Q_R^*(s, a))}{\sum_{b \in \mathcal{A}} \exp(\beta Q_R^*(s, b))},$$

where the inverse temperature  $\beta > 0$  controls the degree of expert optimality.

**Ratings (PDRS).** Ratings provide ordinal feedback in which a human assigns a discrete score to a trajectory reflecting its perceived quality, analogous to Likert-scale judgments ([Likert, 1932](#)). We model this form of feedback using a standard ordinal regression framework, given by the ordered logit model ([McCullagh, 1980](#)).

We assume that each trajectory induces an unobserved latent utility reflecting its quality under the reward function  $R$ , corrupted by stochastic judgment noise. The reported rating  $y \in \{1, \dots, K\}$  generated by discretizing this latent utility via an ordered set of cutpoints  $-\infty < \psi_0 < \psi_1 < \dots < \psi_K < +\infty$ , such that a trajectory  $\xi$  receives rating  $y = k$  whenever its latent utility falls between  $\mu_{k-1}$  and  $\mu_k$ .

Under this model, the likelihood of observing rating  $y = k$  for trajectory  $\xi$  is

$$p(y = k | \xi, R) = F(\psi_k - R(\xi)) - F(\psi_{k-1} - R(\xi)),$$

where  $F$  denotes the logistic cumulative distribution function. Importantly, this feedback modality is not equivalent to direct regression on the reward value, as it only provides ordinal information, but no absolute judgment. The cutpoints  $\{\psi_k\}$  need not be evenly spaced, reflecting the fact that humans typically would not apply uniform or linear thresholds when mapping perceived quality to discrete ratings.

**Stops (PDRS).** Stop signals capture situations in which a human supervisor intervenes to terminate an agent’s behavior once its performance has degraded beyond an acceptable level. Such feedback is ubiquitous in practice, for example, as safety stops in robotics or human-in-the-loop control, yet has received little attention as a learning signal for reward or policy learning. Our framework naturally accommodates stop feedback by modeling it through an explicit likelihood over termination times.

Let  $\tau_{\text{stop}}$  be the (random) time step at which the user intervenes. We model  $\tau_{\text{stop}}$  using a discrete-time hazard model in which the instantaneous hazard at time  $\tau$  depends on the accumulated suboptimality of the trajectory up to that point. Concretely, we define the instantaneous suboptimality of action  $a$  in state  $s$  under reward  $R$  as  $\Delta_R(s, a) = \max_{b \in \mathcal{A}} Q_R^*(s, b) - Q_R^*(s, a)$ , and introduce a backward-looking discount factor  $\rho \in (0, 1]$  that discounts earlier deviations. The resulting hazard function is given by

$$h_R^{\lambda, \rho}(\xi, \tau) = 1 - \exp\left(-\lambda \sum_{t=1}^{\tau} \rho^{\tau-t} \Delta_R(s_t, a_t)\right),$$

Here, the larger  $\lambda > 0$  is, the more unforgiving the expert. We obtain the likelihood of observing a stop at time  $\tau$  as the geometric distribution:

$$p(\tau_{\text{stop}} = \tau | R) = \underbrace{\left[ \prod_{t=1}^{\tau-1} (1 - h_R^{\lambda}(\xi, t)) \right]}_{\text{no stop up until } \tau} h_R^{\lambda}(\xi, \tau). \quad (3)$$

if no stop occurs within the segment, the observation is right-censored.

**Additional Feedback Types.** Other feedback types studied in the literature include *rankings* ([Brown et al., 2019](#); [Myers et al., 2021](#)), *corrections* ([Losey et al., 2022](#)), and other forms of *human intervention* ([Jeon et al., 2020](#)). While we do not explicitly model these here, feedback-specific likelihoods can be derived analogously. Crucially, any such likelihood can be incorporated into our framework and algorithm without additional structural changes. We provide implementation details on feedback simulation in Section [A.2](#).

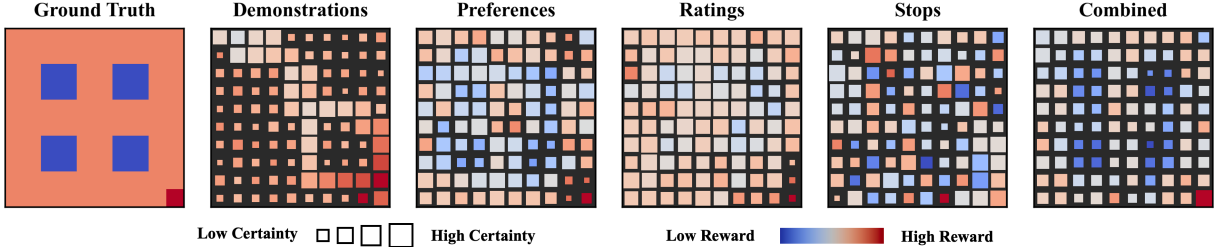


Figure 2: Visualizations of inferred reward functions from 2 demonstrations, 256 pairwise comparisons, or 128 ratings on a  $10 \times 10$  grid\_trap environment. The final column shows the result obtained when combining all feedback modalities.

## 5 MAVRL: Multi-Feedback Amortized Variational Reward Learning

We now present MAVRL, a general learning algorithm for Bayesian reward inference from multiple feedback types. The algorithm instantiates the Bayesian objective introduced in Section 3 using amortized variational inference and directly leverages the feedback-specific likelihood models defined in Section 4.

### 5.1 Objective

We aim to learn a probabilistic reward model together with an auxiliary action-value function that supports feedback types defined in terms of state-action values. Specifically, we parameterize a conditional reward distribution

$$q_\theta(R | s, a, s') = \mathcal{N}(R; \mu_\theta(s, a, s'), \sigma_\theta^2(s, a, s')),$$

where  $\mu_\theta$  and  $\sigma_\theta^2$  are parameterized as neural networks that map tuples  $(s, a, s')$  to a distribution over local reward values. Sampling from this encoder induces a distribution over trajectory returns, which is used to evaluate feedback likelihoods.

In addition, we learn an auxiliary action-value function  $Q_\phi(s, a)$ , which is required by feedback types that depend on value estimates, as well as parameters  $\psi$  associated with feedback-specific likelihood models when applicable, e.g., the cutpoints of the rating model. Crucially, the reward encoder itself is agnostic to the type and structure of feedback; all feedback-specific semantics are captured entirely by the corresponding likelihood functions.

Learning follows directly from the evidence lower bound (ELBO) of the Bayesian reward learning problem. Given feedback datasets  $\mathcal{D}^{(m)}_{m=1}^M$ , where each  $\mathcal{D}^{(m)}$  contains observations of feedback type  $m$ , the unified MAVRL

---

#### Algorithm 1: (MAVRL) Multi-Feedback Amortized Variational Reward Learning

---

```

1 input: Multi-type feedback  $\{\mathcal{D}^{(m)}\}_{m=1}^M$ , hyperparameters  $\lambda_{\text{KL}}, \lambda_{\text{TD}}$ , learning rate  $\eta$ 
2 while not converged do
3   Sample mini-batches for all feedback types:  $\mathcal{B} \leftarrow \{\text{GetBatch}(\mathcal{D}^{(m)})\}_{m=1}^M$ 
4   Encode all transitions:  $(\mu, \sigma^2) \leftarrow q_\theta(\mathcal{B})$ 
5   Reparameterize rewards:  $\mathbf{R} \leftarrow \mu + \sigma \odot \epsilon, \quad \epsilon \sim \mathcal{N}(\mathbf{0}, \mathbf{I})$ 
6   Evaluate  $Q$ -values:  $\mathbf{Q} \leftarrow Q_\phi(\mathcal{B})$ 
7   Compute feedback-specific negative log-likelihoods:  $\{\mathcal{L}_{\text{NLL}}^{(m)}\}_{m=1}^M \leftarrow \{-\log p_\psi^{(m)}(\mathcal{B}^{(m)} | \mathbf{R}, \mathbf{Q})\}_{m=1}^M$ 
8    $\mathcal{L}_{\text{KL}} \leftarrow D_{\text{KL}}(q_\theta \| p)$ , with prior  $p = \mathcal{N}(\mathbf{0}, \mathbf{I})$ 
9    $\mathcal{L}_{\text{TD}} \leftarrow \text{TD}(\mu, \sigma, \mathbf{Q})$ 
10  Aggregate losses:  $\mathcal{L}_{\text{total}} \leftarrow \sum_{m=1}^M \mathcal{L}_{\text{NLL}}^{(m)} + \lambda_{\text{KL}} \mathcal{L}_{\text{KL}} + \lambda_{\text{TD}} \mathcal{L}_{\text{TD}}$ 
11  Update parameters:  $(\theta, \phi) \leftarrow (\theta, \phi) - \eta \nabla_{(\theta, \phi)} \mathcal{L}_{\text{total}}$ 
12 end
13 return reward encoder  $q_\theta$ , action-value model  $Q_\phi$ 

```

---

objective to be maximized is given by

$$\begin{aligned}\mathcal{L}_{\text{MAVRL}}(\theta, \phi, \psi) = & \sum_{m=1}^M \mathbb{E}_{y \sim \mathcal{D}^{(m)}} \left[ \mathbb{E}_{R \sim q_\theta} \left[ \log p_\psi^{(m)}(y | R, Q_\phi) \right] \right] \\ & - \lambda_{\text{KL}} D_{\text{KL}}(q_\theta(R) \| p(R)) + \lambda_{\text{TD}} \mathcal{L}_{\text{TD}}(\theta, \phi).\end{aligned}\quad (4)$$

Here,  $y$  denotes a generic feedback observation whose structure depends on the feedback type, such as a trajectory, a comparison, a scalar rating, or a termination time. Each feedback type contributes a likelihood term to the objective without requiring manual weighting or staged optimization.

The final term  $\mathcal{L}_{\text{TD}}(\theta, \phi)$  enforces consistency between the inferred reward distribution and the auxiliary action-value function. Following [Chan and van der Schaar \(2021\)](#), we include a temporal-difference (TD) regularization term that encourages rewards predicted by the encoder to agree with the one-step Bellman differences implied by  $Q_\phi$ .

To define this term, we leverage the trajectories associated with the observed feedback. Each feedback observation  $o$  is grounded in one or more trajectories, from which we extract state-action transitions. Let  $\tilde{\tau} = (s, a, s', a')$  denote such a transition tuple, where  $a'$  is the action taken in state  $s'$ . The corresponding TD target is defined as

$$\delta_\phi(\tilde{\tau}) := Q_\phi(s, a) - \gamma Q_\phi(s', a').$$

We penalize deviations between this TD target and the reward predicted by the encoder by maximizing its log-likelihood under the encoder distribution,

$$\mathcal{L}_{\text{TD}}(\theta, \phi) = \mathbb{E}_{\tilde{\tau} \sim \mathcal{D}_{\text{traj}}} \left[ \log \mathcal{N}(\delta_\phi(\tilde{\tau}); \mu_\theta(s, a, s'), \sigma_\theta^2(s, a, s')) \right],$$

where  $\mathcal{D}_{\text{traj}}$  denotes the set of transitions extracted from the trajectories underlying the observed feedback.

## 5.2 Properties of MAVRL

**Extensibility.** A central property of MAVRL is that it can incorporate any form of human feedback for which a likelihood can be specified. Each feedback type contributes to the objective exclusively through its likelihood term  $p^{(m)}(y | R, Q_\phi)$ . As a result, extending the framework to a new feedback modality requires only defining an appropriate likelihood, without modifying the reward encoder, the auxiliary value function, or the optimization procedure.

**Unified Objective Without Loss Balancing.** MAVRL does not assume that different feedback modalities share a common intermediate representation or supervision signal. Feedback-specific likelihoods relate observations to the underlying reward through different statistical relationships, such as action probabilities, return comparisons, ordinal thresholds, or cumulative regret. Because all feedback enters through log-likelihood terms in a single variational objective, their relative influence is governed by the assumed noise models rather than manually tuned loss weights. This eliminates the need for staged training, curriculum schedules, or heuristic loss balancing across feedback types.

**Order-Invariant and Asynchronous Training.** The training objective imposes no constraints on the order, frequency, or interleaving of feedback from different modalities. Mini-batches from the type-specific feedback datasets can be sampled independently and combined arbitrarily during optimization.

## 6 Experiments

We evaluate MAVRL across a range of environments and feedback configurations to answer three questions:

- (i) how different feedback types qualitatively complement one another when learning reward functions (Section 6.1),
- (ii) how this complementarity translates into downstream policy performance and reward fidelity (Section 6.2),
- (iii) whether rewards inferred from multi-type feedback lead to more robust behavior under environment perturbations (Section 6.3).

	PDRS	PDRS	PDRS	PDRS	PDRS	PDRS	PDRS	PDRS	PDRS	PDRS
grid_cliff	20.4	62.6	41.3	37.4	16.3	49.5	60.3	41.8	72.2	72.8
grid_sparse	4.9	65.0	35.0	35.0	-0.1	20.0	45.0	35.0	<b>75.0</b>	65.0
grid_trap	49.7	15.6	60.5	56.1	47.1	74.2	64.1	58.3	69.6	<b>76.2</b>
Acrobot-v1	53.3	<b>99.5</b>	<u>97.9</u>	87.6	96.3	96.3	83.0	<b>99.3</b>	97.3	<b>99.0</b>
CartPole-v1	64.7	26.5	69.8	-1.3	66.1	<b>97.7</b>	51.1	62.5	12.2	<u>93.8</u>
LunarLander-v3	-3.8	<b>115.6</b>	3.6	-22.2	30.0	4.0	1.2	38.3	55.7	17.6
										<u>80.4</u>

Table 1: Normalized mean returns ( $n = 10$ ) for different combinations of feedback modalities across environments. Returns are normalized such that 100 corresponds to the performance of an approximately optimal policy trained on the ground-truth reward and 0 corresponds to the performance of a uniformly random policy. Values shown in **bold** are within 1% of the best performance for the corresponding environment, and underlined values indicate the next best result outside this margin.

	PDRS	PDRS	PDRS	PDRS	PDRS	PDRS	PDRS	PDRS	PDRS	PDRS
grid_cliff	0.521	0.646	0.560	0.624	0.512	<b>0.466</b>	0.494	0.592	0.606	0.554
grid_sparse	0.672	<b>0.486</b>	0.569	0.594	0.665	0.645	0.604	0.571	0.511	<u>0.501</u>
grid_trap	0.511	0.697	0.603	0.539	0.491	0.505	<u>0.445</u>	0.608	0.549	0.498
										<b>0.432</b>

Table 2: Mean EPIC distance ( $n = 10$ ) for different combinations of feedback modalities across environments (lower is better). Values in **bold** are the best for the corresponding environment, and underlined values indicate the next best result outside this margin.

Our experiments span both tabular grid-world domains and continuous-control benchmarks, and consider demonstrations, pairwise comparisons, ratings, and stop feedback both in isolation and in combination.

Unless otherwise stated, all methods are trained under a fixed feedback budget per environment, with identical numbers of feedback samples allocated to each modality to enable fair comparison. Let  $n_p$ ,  $n_d$ ,  $n_r$ , and  $n_s$  denote the numbers of preferences, demonstrations, ratings, and stop signals, respectively. In the grid-world environments, we set  $n_p = n_r = 64$ ,  $n_d = 1$ , and  $n_s = 256$ . In Acrobot-v1 and CartPole-v1, we set  $n_p = n_r = 256$ ,  $n_d = 4$ , and  $n_s = 64$ . In LunarLander-v3, we set  $n_p = n_r = 1024$ ,  $n_d = 32$ , and  $n_s = 256$ . Additional results for alternative feedback budgets are reported in Section E.

## 6.1 Feedback Types Complement One Another

In Figure 2, we visualize reward estimates learned with MAVRL based on different individual feedback types and their combination in a grid-world environment. We report both the learned mean reward estimate and its corresponding uncertainty, quantified by the variance. Additional examples can be found in Section D.

We find that each feedback type induces a characteristic pattern in the inferred reward and uncertainty estimates. Demonstrations yield low-uncertainty reward estimates along expert trajectories, but leave large regions of the state space underdetermined. Pairwise preferences provide broader coverage, but can assign a high reward to frequently visited intermediate states that are not globally optimal. Ratings reliably identify the goal state, but offer limited information about the surrounding reward landscape. Stop feedback strongly constrains unsafe or low-reward regions, while providing relatively little guidance on desirable behavior beyond avoidance.

Illustrating the complementary nature of different types of feedback, these limitations are mitigated when they are combined. Our reward model, trained on combined feedback, can reconstruct the original ground-truth reward function with high fidelity and reliably identify both high- and low-reward states.

## 6.2 Combining Feedback Improves Policy Performance and Reward Identification

We evaluate the downstream policy performance of different feedback combinations across a range of grid-world and continuous-control environments in Table 1. For each combination, we optimize a policy w.r.t. the learned reward estimate and report the policy’s total return w.r.t. the ground-truth reward function.

All results are averaged over 10 runs, and the returns are linearly scaled per environment so that 100 corresponds to an approximately optimal policy trained on the ground-truth reward and 0 corresponds to the return of a uniformly random policy. Hence, values exceeding 100 indicate that the learned policy outperforms the policy trained on the ground-truth reward.

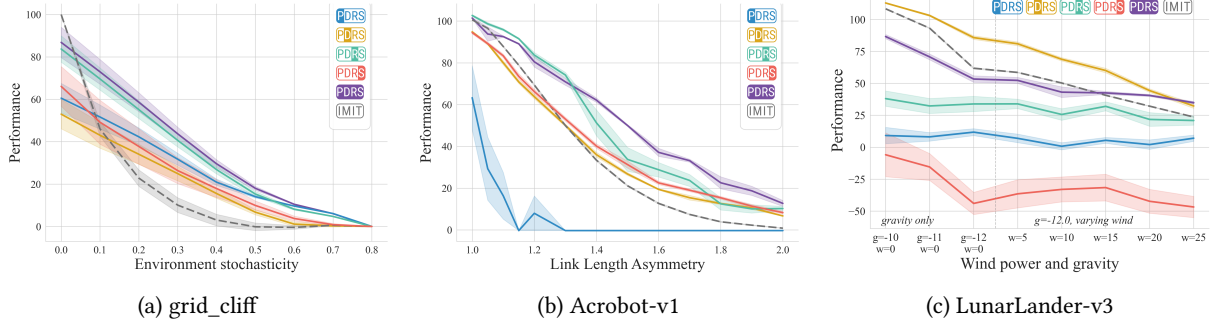


Figure 3: Normalized mean returns ( $n = 10$ ) of policies trained on rewards inferred by each method under three dynamics perturbation scenarios. Reward models and baselines are trained in the unperturbed setting and remain fixed throughout the variations. Error bars denote standard error. (a) Increasing environmental stochasticity in grid\_cliff. (b) Increasing ratio between pendulum handle lengths in Acrobot-v1. (c) Increasing gravity and wind-power in LunarLander-v3.

While these normalized metrics capture downstream policy performance, they do not globally reflect reward recovery. To assess this, Table 2 reports the EPIC distance (Gleave et al., 2021), which is zero for reward functions that are equivalent up to potential-based shaping, positive scaling, and constant shifts. We report EPIC distance only for tabular environments, where exact reward comparisons are feasible.

**Combining all feedback types yields the strongest overall performance.** Overall, **PDRS** performs consistently strongly across environments, achieving either the best performance or results within 1% of the best in five out of six environments, with the exception of CartPole-v1. This supports our central hypothesis that MAVRL is capable of leveraging complementary information captured in different feedback types.

**No single-type baselines dominates across all environments.** Perhaps unsurprisingly, demonstrations (**PDRS**) excel in sparse reward settings, such as grid\_sparse (65.0) and LunarLander-v3 (115.6), while ratings (**PDRS**) perform best in Acrobot-v1 (97.9) among the single feedback type approaches. Preferences (**PDRS**) show relatively modest performance as a standalone modality, yet contribute substantially when combined with others, consistent with prior findings that pairwise comparisons require large quantities to achieve competitive performance (Christiano et al., 2017).

**Stop feedback complements other feedback.** In several environments, combinations involving stop feedback (**PDRS**, **PDRS**, **PDRS**) generally outperform their non-stop counterparts. For instance, in grid\_cliff, **PDRS** (72.2) improves over **PDRS** alone (62.6), and **PDRS** (72.8) similarly improves over **PDRS** (41.3). This suggests that stop signals provide valuable information about the suboptimality of trajectories that is otherwise difficult to obtain from other feedback.

**EPIC distance reveals reward recovery quality beyond policy performance.** Table 2 shows that low EPIC distance (indicating faithful reward recovery) does not always align with high downstream policy performance. In grid\_sparse, **PDRS** achieves the lowest EPIC distance (0.486), yet **PDRS** yields the best performing policy. Notably, the combination of all feedback types, **PDRS**, achieves either the best or second-best EPIC distance in two of three tabular environments (grid\_cliff: 0.468; grid\_trap: 0.432), suggesting that combining feedback modalities does improve reward recovery in addition to policy performance.

**Some feedback combinations underperform compared to their constituent modalities.** In CartPole-v1, **PDRS** (12.2) significantly underperforms ratings alone (**PDRS**, 69.8), and combinations that include stop feedback generally struggle in this environment. Similarly, **PDRS** occasionally underperforms single modalities (e.g., in grid\_cliff: **PDRS** 16.3 vs. **PDRS** 20.4), suggesting potential conflicts between demonstration-derived and preference-derived gradients that warrant further investigation. In the sparse reward setting of LunarLander-v3, where local reward signals can be misleading, **PDRS** does not match the performance of standalone **PDRS**, indicating that in such regimes, additional feedback modalities may introduce additional noise rather than a complementary signal. Nevertheless, within LunarLander-v3, all remaining individual feedback types are outperformed by the combinations of feedback.

### 6.3 Rewards Learned from Multi-Type Feedback are More Robust

We evaluate the robustness of rewards learned from different feedback modalities under systematic perturbations of the environment dynamics. For each feedback configuration, we fix reward models trained in the unperturbed setting and retrain policies in the perturbed environments without further reward adaptation. We compare individual feedback modalities, their combination (PDRS), and a behavioral cloning baseline (IMIT). Full experimental details and results for all feedback combinations are provided in Section C.

**Results.** Across all environments, policies trained on rewards inferred from multiple feedback types (PDRS) degrade more gracefully under perturbations than those trained from individual feedback modalities or imitation alone.

In the grid-world setting (Figure 3a), increasing action stochasticity causes imitation and single-feedback reward models, such as PDRS, PDRS, and PDRS, to deteriorate rapidly, whereas rewards learned from combined feedback maintain higher mean returns.

A similar pattern is observed in Acrobot (Figure 3b), where structural changes to the system dynamics disproportionately affect the imitated policy and the single-feedback reward models, while combined feedback yields consistently more stable performance across perturbation levels.

In LunarLander-v3 (Figure 3c), perturbations to gravity and wind severely degrade the performance of IMIT. In contrast, MAVRL, especially when trained with multi-type feedback (PDRS), remains significantly more robust under increasingly challenging dynamics.

## 7 Conclusion

We framed reward learning from multiple feedback types as Bayesian inference over a shared latent reward function, where each feedback modality contributes through an explicit likelihood, and proposed MAVRL, a scalable amortized variational inference algorithm that optimizes a single unified objective. Empirically, we found that different feedback types induce distinct reward and uncertainty structures, and jointly inferring rewards from multiple modalities can exploit their complementary strengths, improving reward recovery, downstream policy performance, and robustness.

**Limitations.** Our evaluation is limited to simulated environments, which, while allowing controlled analysis of different feedback types, do not capture the full complexity of real-world tasks. In addition, we rely on synthetically generating feedback, and applying MAVRL to real human feedback, which may exhibit systematic biases, inconsistencies, or context-dependent judgments, remains an important direction for future work. Finally, while our framework infers reward uncertainty, we do not yet exploit this uncertainty for guiding feedback collection, leaving active learning of heterogeneous feedback as a promising avenue for future work.

## Acknowledgments

This research was primarily supported by the ETH AI Center through an ETH AI Center doctoral fellowship to Raphaël Baur and an ETH AI Center postdoctoral fellowship to Thomas Kleine Buening.

## References

- Pieter Abbeel and Andrew Y. Ng. Apprenticeship learning via inverse reinforcement learning. In *Proceedings of the twenty-first international conference on Machine learning*, page 1, New York, NY, USA, July 2004. Association for Computing Machinery. ISBN 978-1-58113-838-2. doi: 10.1145/1015330.1015430. URL <https://dl.acm.org/doi/10.1145/1015330.1015430>.
- Ahmed Abouelazm, Jonas Michel, and J. Marius Zöllner. A review of reward functions for reinforcement learning in the context of autonomous driving. In *2024 IEEE Intelligent Vehicles Symposium (IV)*, pages 156–163, 2024. doi: 10.1109/IV55156.2024.10588385.
- Dario Amodei, Chris Olah, Jacob Steinhardt, Paul Christiano, John Schulman, and Dan Mané. Concrete problems in AI safety. *arXiv preprint arXiv:1606.06565*, 2016.

Andrea Bajcsy, Dylan P. Losey, Marcia K. O’Malley, and Anca D. Dragan. Learning robot objectives from physical human interaction. In Sergey Levine, Vincent Vanhoucke, and Ken Goldberg, editors, *Proceedings of the 1st Annual Conference on Robot Learning*, volume 78 of *Proceedings of Machine Learning Research*, pages 217–226. PMLR, 13–15 Nov 2017. URL <https://proceedings.mlr.press/v78/bajcsy17a.html>.

Daniel Brown, Wonjoon Goo, Prabhat Nagarajan, and Scott Niekum. Extrapolating beyond suboptimal demonstrations via inverse reinforcement learning from observations. In Kamalika Chaudhuri and Ruslan Salakhutdinov, editors, *Proceedings of the 36th International Conference on Machine Learning*, volume 97 of *Proceedings of Machine Learning Research*, pages 783–792. PMLR, 09–15 Jun 2019.

Daniel S. Brown, Russell Coleman, Ravi Srinivasan, and Scott Niekum. Safe imitation learning via fast bayesian reward inference from preferences. In *Proceedings of the 37th International Conference on Machine Learning*, ICML’20. JMLR.org, 2020.

Erdem Biyik, Dylan P. Losey, Malayandi Palan, Nicholas C. Landolfi, Gleb Shevchuk, and Dorsa Sadigh. Learning reward functions from diverse sources of human feedback: Optimally integrating demonstrations and preferences. *The International Journal of Robotics Research*, 41(1):45–67, January 2022. ISSN 0278-3649. doi: 10.1177/02783649211041652. URL <https://doi.org/10.1177/02783649211041652>. Publisher: SAGE Publications Ltd STM.

Yuang Cai, Yuyu Yuan, Jinsheng Shi, and Qinhong Lin. Approximated variational bayesian inverse reinforcement learning for large language model alignment. In *Proceedings of the AAAI Conference on Artificial Intelligence*, volume 39, pages 23505–23513, 2025.

Alex James Chan and Mihaela van der Schaar. Scalable Bayesian inverse reinforcement learning. In *International Conference on Learning Representations 2021*, 2021. URL <https://openreview.net/forum?id=4qR3coiNaIV>.

Paul F. Christiano, Jan Leike, Tom B. Brown, Miljan Martic, Shane Legg, and Dario Amodei. Deep reinforcement learning from human preferences. In *Proceedings of the 31st International Conference on Neural Information Processing Systems*, NIPS’17, pages 4302–4310, Red Hook, NY, USA, December 2017. Curran Associates Inc. ISBN 978-1-5108-6096-4.

Samuel J Gershman and Yael Niv. Novelty and inductive generalization in human reinforcement learning. *Topics in cognitive science*, 7(3):391–415, 2015.

Gaurav R. Ghosal, Matthew Zurek, Daniel S. Brown, and Anca D. Dragan. The effect of modeling human rationality level on learning rewards from multiple feedback types. In *Proceedings of the Thirty-Seventh AAAI Conference on Artificial Intelligence and Thirty-Fifth Conference on Innovative Applications of Artificial Intelligence and Thirteenth Symposium on Educational Advances in Artificial Intelligence*. AAAI Press, 2023. ISBN 978-1-57735-880-0. doi: 10.1609/aaai.v37i5.25740. URL <https://doi.org/10.1609/aaai.v37i5.25740>.

Adam Gleave, Michael D Dennis, Shane Legg, Stuart Russell, and Jan Leike. Quantifying differences in reward functions. In *International Conference on Learning Representations*, 2021. URL <https://openreview.net/forum?id=LwEQnp6CYev>.

Dylan Hadfield-Menell, Anca Dragan, Pieter Abbeel, and Stuart Russell. The off-switch game. In *Proceedings of the 26th International Joint Conference on Artificial Intelligence*, IJCAI’17, page 220–227. AAAI Press, 2017. ISBN 9780999241103.

Dan Hendrycks, Nicholas Carlini, John Schulman, and Jacob Steinhardt. Unsolved problems in ML safety. *arXiv preprint arXiv:2109.13916*, 2021.

Borja Ibarz, Jan Leike, Tobias Pohlen, Geoffrey Irving, Shane Legg, and Dario Amodei. Reward learning from human preferences and demonstrations in Atari. *Advances in Neural Information Processing Systems*, 31, 2018.

Hong Jun Jeon, Smitha Milli, and Anca D. Dragan. Reward-rational (implicit) choice: A unifying formalism for reward learning, December 2020. URL <http://arxiv.org/abs/2002.04833>. arXiv:2002.04833 [cs].

Diederik P. Kingma and Max Welling. Auto-Encoding Variational Bayes. In *2nd International Conference on Learning Representations, ICLR 2014, Banff, AB, Canada, April 14-16, 2014, Conference Track Proceedings*, 2014. doi: 10.48550/arXiv.1312.6114.

W. Bradley Knox and Peter Stone. Interactively shaping agents via human reinforcement: The TAMER framework. In *Proceedings of the fifth international conference on Knowledge capture*, K-CAP '09, pages 9–16, New York, NY, USA, September 2009. Association for Computing Machinery. ISBN 978-1-60558-658-8. doi: 10.1145/1597735.1597738. URL <https://dl.acm.org/doi/10.1145/1597735.1597738>.

W Bradley Knox, Alessandro Allievi, Holger Banzhaf, Felix Schmitt, and Peter Stone. Reward (mis) design for autonomous driving. *Artificial Intelligence*, 316:103829, 2023.

Rensis Likert. A technique for the measurement of attitudes. *Archives of Psychology*, 140:1–55, 1932.

Dylan P. Losey, Andrea Bajcsy, Marcia K. O’Malley, and Anca D. Dragan. Physical interaction as communication: Learning robot objectives online from human corrections. *The International Journal of Robotics Research*, 41(1): 20–44, 2022. doi: 10.1177/02783649211050958. URL <https://doi.org/10.1177/02783649211050958>.

Ilya Loshchilov and Frank Hutter. Fixing weight decay regularization in adam. *CoRR*, abs/1711.05101, 2017. URL <http://arxiv.org/abs/1711.05101>.

MaÃÂgi Macuglia, Paul Friedrich, and Giorgia Ramponi. Fine-tuning behavioral cloning policies with preference-based reinforcement learning. *arXiv preprint arXiv:2509.26605*, 2025.

Peter McCullagh. Regression models for ordinal data. *Journal of the Royal Statistical Society: Series B (Methodological)*, 42(2):109–127, 1980. doi: <https://doi.org/10.1111/j.2517-6161.1980.tb01109.x>.

Shaunak A. Mehta and Dylan P. Losey. Unified learning from demonstrations, corrections, and preferences during physical human–robot interaction. *J. Hum.-Robot Interact.*, 13(3), August 2024. doi: 10.1145/3623384. URL <https://doi.org/10.1145/3623384>.

Yannick Metz, David Lindner, RaphaÃÂl Baur, Daniel A. Keim, and Mennatallah El-Assady. RLHF-Blender: A Configurable Interactive Interface for Learning from Diverse Human Feedback. In *Interactive Learning with Implicit Human Feedback Workshop at ICML*, Honolulu, Hawaii, USA, 2023. doi: 10.48550/ARXIV.2308.04332.

Yannick Metz, Andras Geiszl, RaphaÃÂl Baur, and Mennatallah El-Assady. Reward learning from multiple feedback types. *International Conference on Learning Representations*, 2025. URL <https://openreview.net/forum?id=9Ieq8jQNA1>.

Vivek Myers, Erdem Biyik, Nima Anari, and Dorsa Sadigh. Learning Multimodal Rewards from Rankings. *Conference on Robot Learning (CoRL) 2021*, October 2021. doi: 10.48550/arXiv.2109.12750. URL <http://arxiv.org/abs/2109.12750>.

Andrew Y. Ng, Daishi Harada, and Stuart J. Russell. Policy invariance under reward transformations: Theory and application to reward shaping. In *Proceedings of the 16th International Conference on Machine Learning*, 1999.

Andrew Y Ng, Stuart Russell, et al. Algorithms for inverse reinforcement learning. In *Icml*, volume 1, page 2, 2000.

Long Ouyang, Jeff Wu, Xu Jiang, Diogo Almeida, Carroll L. Wainwright, Pamela Mishkin, Chong Zhang, Sandhini Agarwal, Katarina Slama, Alex Ray, John Schulman, Jacob Hilton, Fraser Kelton, Luke Miller, Maddie Simens, Amanda Askell, Peter Welinder, Paul Christiano, Jan Leike, and Ryan Lowe. Training language models to follow instructions with human feedback, March 2022. URL <http://arxiv.org/abs/2203.02155>. arXiv:2203.02155 [cs].

Malayandi Palan, Nicholas C Landolfi, Gleb Shevchuk, and Dorsa Sadigh. Learning reward functions by integrating human demonstrations and preferences. *Robotics: Science and Systems 2019*, 2019. URL <https://www.roboticsproceedings.org/rss15/p23.pdf>.

Adam Paszke, Sam Gross, Francisco Massa, Adam Lerer, James Bradbury, Gregory Chanan, Trevor Killeen, Zeming Lin, Natalia Gimelshein, Luca Antiga, Alban Desmaison, Andreas Köpf, Edward Z. Yang, Zach DeVito, Martin Raison, Alykhan Tejani, Sasank Chilamkurthy, Benoit Steiner, Lu Fang, Junjie Bai, and Soumith Chintala. Pytorch: An imperative style, high-performance deep learning library. *CoRR*, abs/1912.01703, 2019. URL <http://arxiv.org/abs/1912.01703>.

Sriyash Poddar, Yanming Wan, Hamish Ivison, Abhishek Gupta, and Natasha Jaques. Personalizing reinforcement learning from human feedback with variational preference learning. In *Proceedings of the 38th International Conference on Neural Information Processing Systems*, NIPS '24, Red Hook, NY, USA, 2024. Curran Associates Inc. ISBN 9798331314385.

Antonin Raffin, Ashley Hill, Adam Gleave, Anssi Kanervisto, Maximilian Ernestus, and Noah Dormann. Stable-baselines3: Reliable reinforcement learning implementations. *Journal of Machine Learning Research*, 22(268):1–8, 2021. URL <http://jmlr.org/papers/v22/20-1364.html>.

Deepak Ramachandran and Eyal Amir. Bayesian inverse reinforcement learning. In *Proceedings of the 20th international joint conference on Artificial intelligence*, IJCAI’07, pages 2586–2591, San Francisco, CA, USA, January 2007. Morgan Kaufmann Publishers Inc.

Constantin A Rothkopf and Christos Dimitrakakis. Preference elicitation and inverse reinforcement learning. In *Joint European conference on machine learning and knowledge discovery in databases*, pages 34–48. Springer, 2011.

Christian Wirth, Johannes Fürnkranz, and Gerhard Neumann. Model-free preference-based reinforcement learning. In *Proceedings of the Thirtieth AAAI Conference on Artificial Intelligence*, AAAI’16, pages 2222–2228, Phoenix, Arizona, February 2016. AAAI Press.

Yifu Yuan, Jianye Hao, Yi Ma, Zibin Dong, Hebin Liang, Jinyi Liu, Zhixin Feng, Kai Zhao, and Yan Zheng. Uni-RLHF: Universal platform and benchmark suite for reinforcement learning with diverse human feedback. In *The Twelfth International Conference on Learning Representations, ICLR*, 2024. URL <https://openreview.net/forum?id=WesY0H9ghM>.

## A Implementation Details

### A.1 Model Architecture

The reward encoder  $q_\theta$  and Q-value estimator  $Q_\phi$  were implemented as two-layer MLPs with Leaky ReLU activations. For grid environments, we used 64 hidden units per layer, learning rate  $5 \times 10^{-4}$ , batch size 32, and state-only rewards  $R(s)$ . For control tasks (CartPole-v1, Acrobot-v1, LunarLander-v3), we used 256 hidden units per layer, learning rate  $10^{-4}$ , batch size 128, and state-action rewards  $R(s, a)$ . All models were trained using AdamW with gradient clipping (max norm 1.0) (Loshchilov and Hutter, 2017). The reward encoder parameterizes a Gaussian posterior with a standard normal prior, trained via the reparameterization trick. Expert reference policies were trained with StableBaseline3’s DQN implementation (all except LunarLander-v3) and PPO implementation (LunarLander-v3) (Raffin et al., 2021). For each environment and feedback combination, we treat  $\lambda_{\text{TD}}$  and  $\lambda_{TD}$  as hyperparameters and select the best-performing setting from  $\{0.5, 1.0\}$  using the same tuning procedure applied uniformly to all methods. Model and training code was implemented with PyTorch (Paszke et al., 2019). The source code is supplied as supplementary material.

### A.2 Feedback Simulation

We simulate human feedback from trajectories collected by rolling out Boltzmann-rational policies with temperature parameter  $\beta_{\text{traj}}$ . Below we describe the generation process for each feedback type.

**Preferences.** We extract random segments of fixed length  $L$  from collected trajectories. For each pair of segments  $(\xi_1, \xi_2)$ , we compute their normalized returns  $\bar{R}(\xi_i) = R(\xi_i)/L$  and generate a preference according to the Bradley-Terry model:

$$p(\xi_1 \succ \xi_2) = \sigma(\beta_{\text{pref}} \cdot (\bar{R}(\xi_1) - \bar{R}(\xi_2))),$$

where  $\sigma$  denotes the logistic sigmoid and  $\beta_{\text{pref}}$  controls preference rationality. The observed preference is sampled as a Bernoulli random variable with this probability. We choose  $\beta_{\text{pref}} = 5.0$ , segment length  $L = 10$ , for grids and  $L = 32$  for all other environments, trajectory rationality  $\beta_{\text{traj}} = 0.0$  for grids (uniform policy), 5.0 for all other environments.

**Demonstrations.** Expert demonstrations are generated by rolling out a Boltzmann-rational policy  $\pi(a | s) \propto \exp(\beta_{\text{demo}} \cdot Q^*(s, a))$ , where  $Q^*$  denotes the optimal Q-function. The demonstration rationality  $\beta_{\text{demo}}$  controls the degree of expert optimality. We choose  $\beta_{\text{demo}} = 10.0$  for grids,  $\beta_{\text{demo}} = 5.0$  for all remaining environments.

**Ratings.** We extract random segments from trajectories and compute their normalized returns. Ordinal ratings are assigned using quantile-based cutpoints: given  $K$  rating categories, we compute the  $(100 \cdot k/K)$ -th percentile of segment returns for  $k \in \{1, \dots, K-1\}$  as cutpoints  $\{\mu_k\}$ . A segment with return  $R$  receives rating  $y = k$  if  $\mu_{k-1} < R \leq \mu_k$ . This ensures approximately balanced categories. Typical parameters:  $K = 5$  categories, segment length  $L \in \{10, 32\}$  (grids, all other environments), trajectory rationality  $\beta_{\text{traj}} \in \{0.0, 1.0, 5.0\}$  (grids, Acrobot-v1 and CartPole-v1, LunarLander-v3 respectively).

**Stops.** We simulate stop feedback using a discrete-time hazard model based on cumulative regret. For a trajectory segment, we compute the instantaneous regret at each time step as  $\Delta_t = \max_b Q^*(s_t, b) - Q^*(s_t, a_t)$  and maintain a discounted cumulative regret:

$$\mathcal{R}_t = \rho \mathcal{R}_{t-1} + \Delta_t,$$

where  $\rho \in [0, 1]$  is the regret discount factor controlling how quickly past suboptimality is “forgotten”. The hazard rate (probability of stopping at time  $t$  given no prior stop) is:

$$h_t = 1 - \exp(-\lambda \mathcal{R}_t).$$

The sensitivity parameter  $\lambda$  is calibrated from the data as  $\lambda = c/\mathcal{R}_{\text{ref}}$ , where  $c$  is a scaling constant and  $\mathcal{R}_{\text{ref}}$  is a reference regret level (typically the 50th percentile of maximum cumulative regrets across segments). Larger  $c$  yields more aggressive stopping behavior. Stop times are sampled sequentially: at each time step  $t$ , we sample a stop event with probability  $h_t$ . If no stop occurs within the segment, the observation is right-censored. Parameters:  $c = 1.0$ , regret discount  $\rho = 0.1$ , reference percentile = 50%, segment length  $L \in \{10, 32\}$  (grids, all remaining environments), trajectory rationality  $\beta_{\text{traj}} \in \{0.0, 1.0\}$ .

## B Hardware and Computational Resources

Due to the large number of evaluated configurations in Section 6, individual reward model training and evaluation runs were distributed on a SLURM-managed institutional cluster, with each worker allocated 4 CPU cores and 8 GB of RAM. Due to the small size of the reward encoder and Q-value estimator networks, no GPU acceleration was required. For the final experiments, the total compute consumption amounted to approximately  $2.7 \times 10^5$  CPU-hours.

We note that an *individual* reward model training run takes approximately 2 minutes for the grid environments and about 15 minutes for all other environments on a single machine, with most of the computation time spent on retraining a policy using the inferred reward function for evaluation.

## C Additional Transfer Results and Detailed Perturbation Description

Transfer performance results for all feedback combinations are shown in Figure 4. We now summarize the environmental perturbations used to evaluate the robustness of downstream policy performance under systematic changes in environment dynamics.

**Grid-World Environments (grid\_cliff, grid\_sparse, grid\_trap).** For the grid-world environments, we perturb the transition dynamics by introducing stochasticity in the agent’s action execution. Specifically, we increase the probability of taking a random action  $p_{\text{rand}} \in [0, 0.8]$ , where  $p_{\text{rand}} = 0$  corresponds to deterministic dynamics. These environments feature sparse rewards and punishing regions such as cliffs or traps, making robustness to action noise particularly important.

In the grid-world experiments, all methods converge to the same performance as  $p_{\text{rand}} \rightarrow 0.8$ . This behavior follows directly from how random actions are defined.

Let  $a^*$  denote the action selected by a deterministic policy  $\pi$ , such that  $\pi(a^* | s) = 1$ . Under action noise with probability  $p_{\text{rand}}$ , the executed policy becomes

$$\pi_{\text{rand}}(a^* | s) = 1 - p_{\text{rand}}, \quad \pi_{\text{rand}}(a' | s) = \frac{p_{\text{rand}}}{|\mathcal{A}| - 1} \quad \text{for } a' \neq a^*.$$

In the grid environments with  $|\mathcal{A}| = 5$ , setting  $p_{\text{rand}} = 0.8$  yields  $\pi_{\text{rand}}(a | s) = 0.2$  for all actions  $a$ , which is equivalent to a uniform random policy. Since returns are normalized such that the uniform policy achieves a value of 0.0, all methods converge to this value at  $p_{\text{rand}} = 0.8$ .

For larger values of  $p_{\text{rand}}$ , unintended actions receive higher probability mass than the originally intended action, rendering deterministic action selection suboptimal. We therefore restrict our analysis to  $p_{\text{rand}} \leq 0.8$ .

**LunarLander-v3.** For LunarLander-v3, we perturb the dynamics by jointly increasing the magnitude of gravity and the strength of wind. Concretely, we vary the gravity parameter in  $\{-10.0, -11.0, -12.0\}$ , with default value  $-10.0$ , and the wind power in  $[0.0, 25.0]$ , with default value  $0.0$ . These perturbations induce increasingly challenging dynamics that require the agent to mitigate rapid descents caused by stronger gravity while compensating for lateral drift induced by wind.

**Acrobot-v1.** For Acrobot-v1, we perturb the system by varying the ratio between the two link lengths of the double pendulum. Increasing asymmetry between the links alters the inertia and coupling of the system, resulting in progressively different and more challenging dynamics compared to the unperturbed setting.

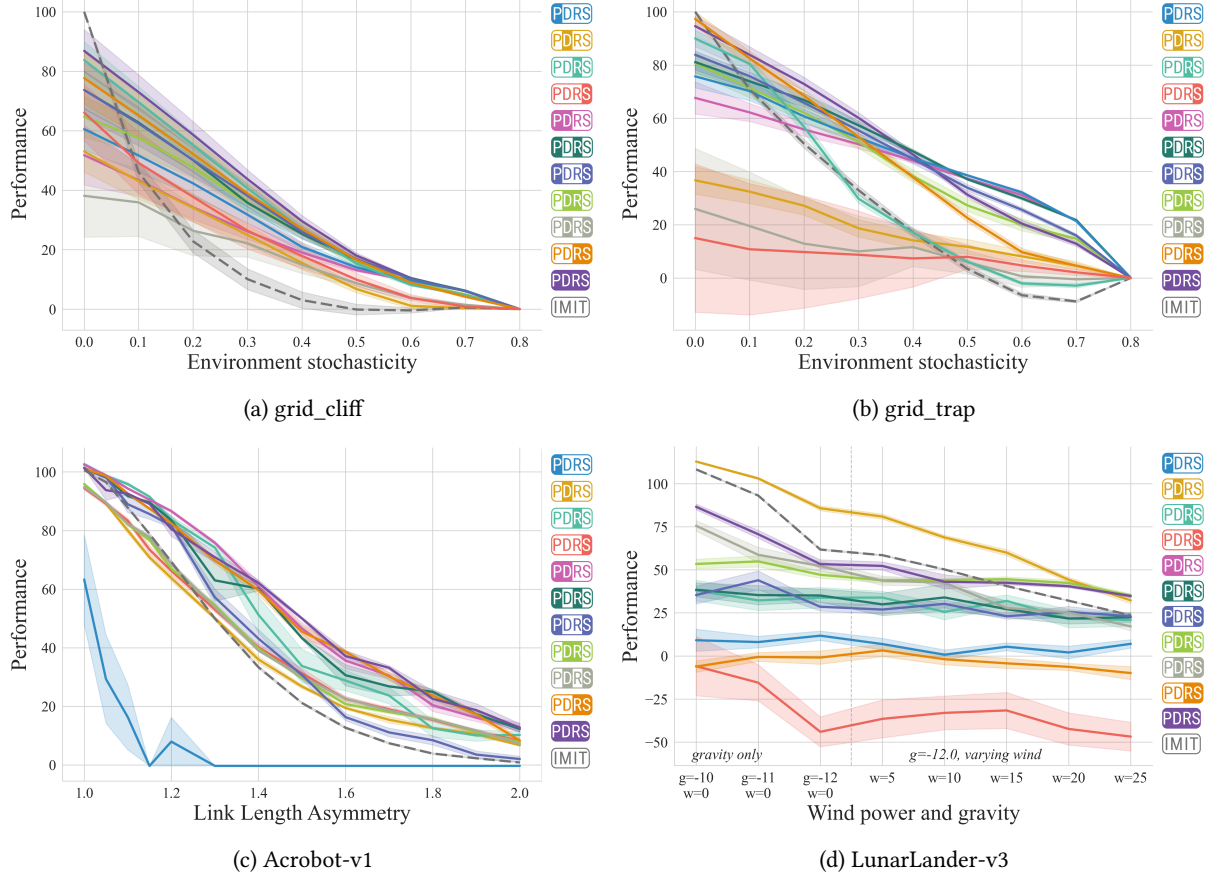


Figure 4: Normalized mean returns ( $n = 10$ ) of policies trained on rewards inferred by each method under three dynamics perturbation scenarios. Reward models and baselines are trained in the unperturbed setting and remain fixed throughout the variations. Returns are normalized such that 100.0 corresponds to the performance of an approximately optimal policy trained on the ground-truth reward *in the unperturbed setting* and, analogously, 0.0 corresponds to the performance of a uniformly random policy. Error bars denote standard error. (a) and (b) Increasing environmental stochasticity in grid\_cliff and grid\_trap. (c) Increasing gravity and wind-power in LunarLander-v3. (d) Increasing ratio between pendulum handle lengths in Acrobot-v1.

## D Additional Qualitative Results

In the following section, we present additional qualitative results for all grid environments. Figures 5 to 7 each show two visualizations of the same inferred reward models: (a) a joint visual encoding of mean and variance, consistent with Figure 2, and (b) a separate visual encoding of mean and variance.

Note that we linearly normalize the inferred reward values per feedback type. This would not affect policy performance, since the induced behavior of the optimal policy is invariant to positive scaling and constant shifts of the reward function (Ng et al., 1999).

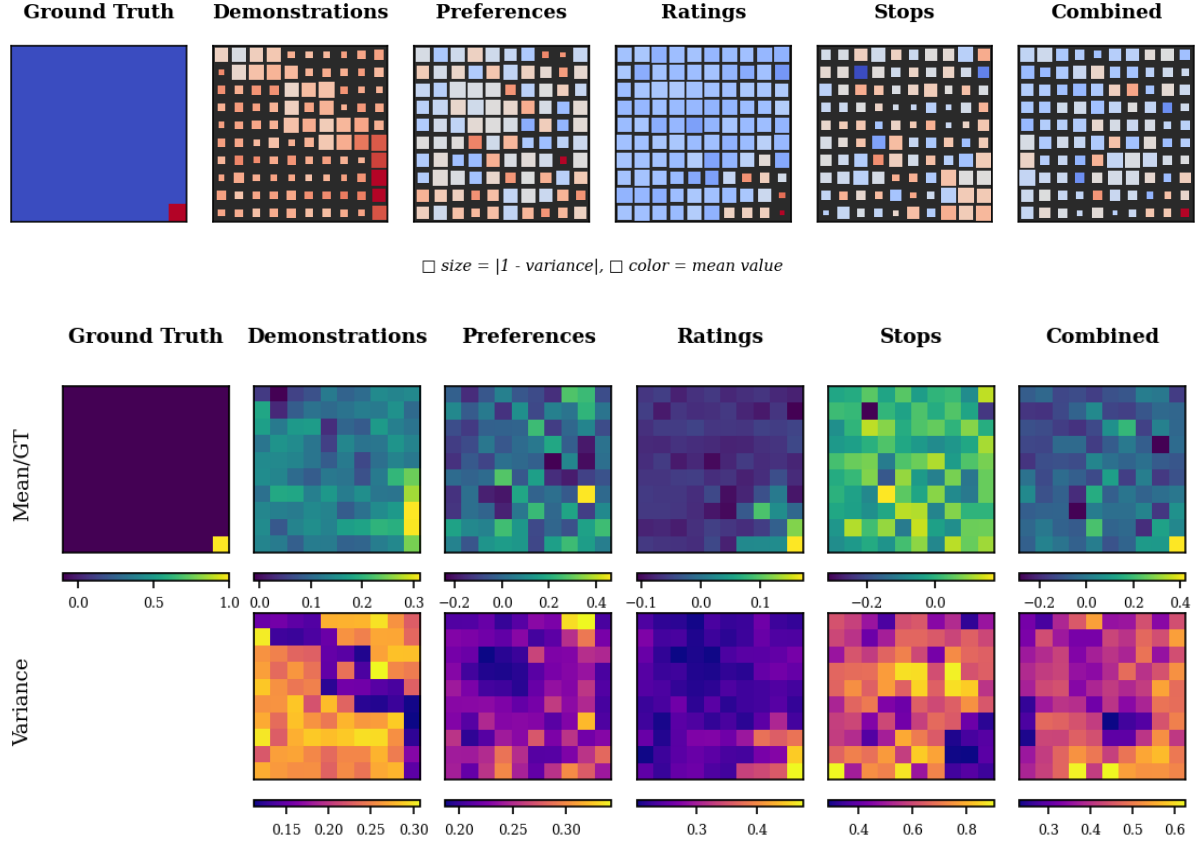


Figure 5: **grid\_spare**: Visualizations of inferred reward functions from 2 demonstrations, 256 pairwise comparisons, or 128 ratings on a  $10 \times 10$  grid\_spare environment. The final column shows the result obtained when combining all feedback modalities. (a) Joint visual encoding of mean and variance. (b) Separate visual encoding of mean and variance for the same data. The rightmost column shows the result obtained when combining all feedback modalities.

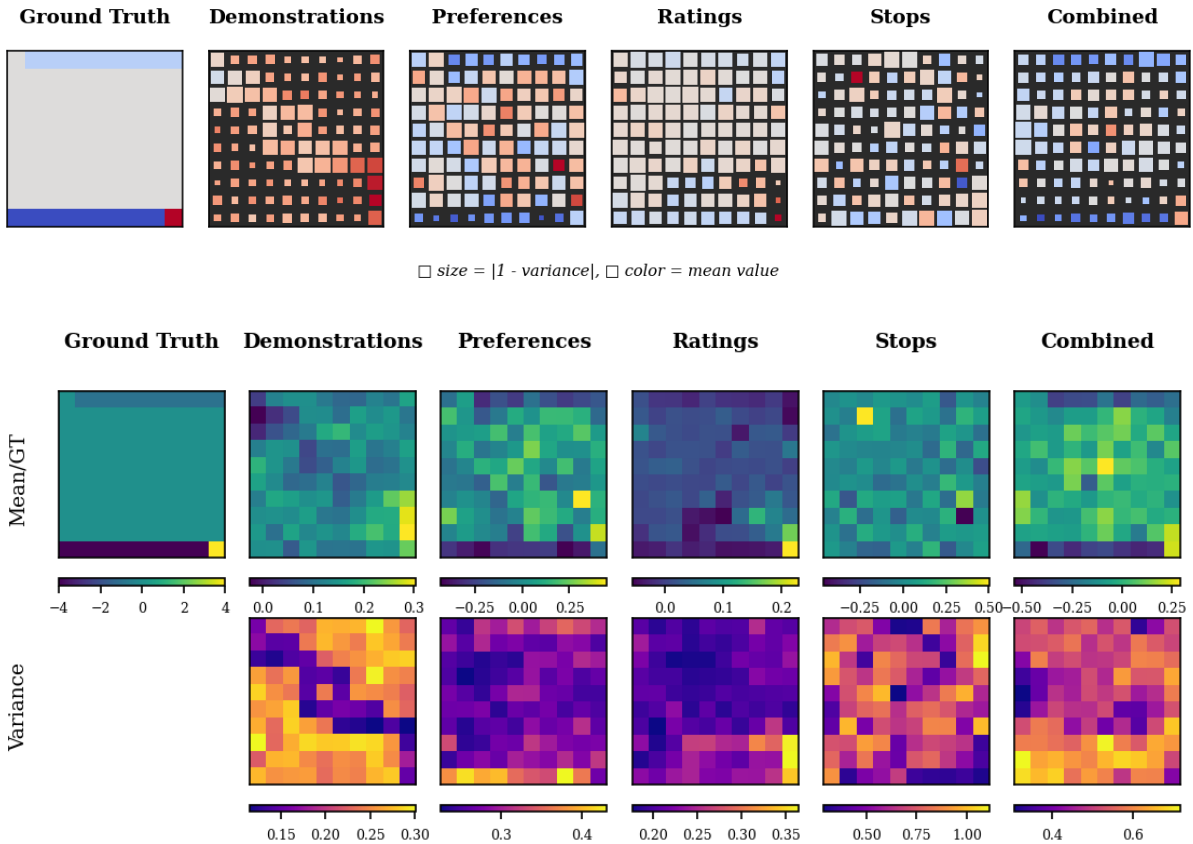


Figure 6: **grid\_cliff**: Visualizations of inferred reward functions from 2 demonstrations, 256 pairwise comparisons, or 128 ratings on a  $10 \times 10$  grid\_cliff environment. The final column shows the result obtained when combining all feedback modalities. (a) Joint visual encoding of mean and variance. (b) Separate visual encoding of mean and variance for the same data. The rightmost column shows the result obtained when combining all feedback modalities.

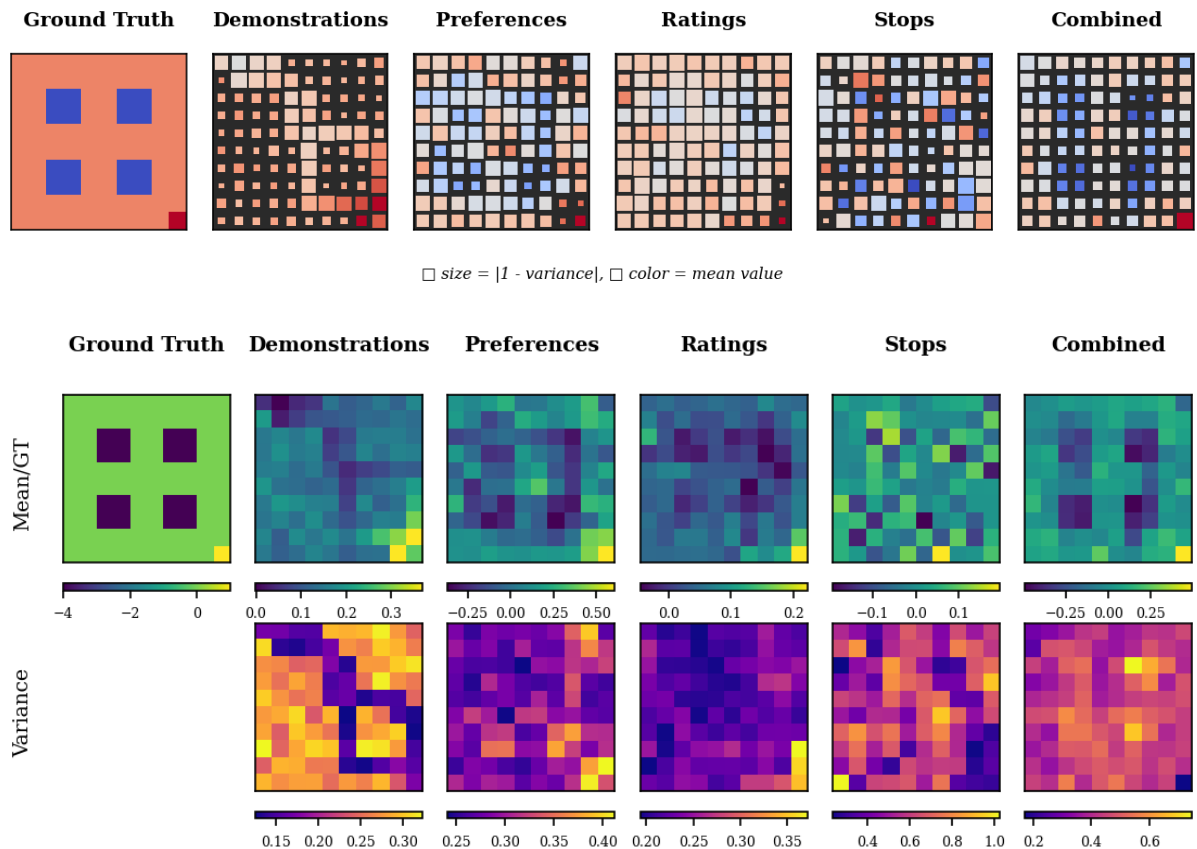


Figure 7: **grid\_trap**: Visualizations of inferred reward functions from 2 demonstrations, 256 pairwise comparisons, or 128 ratings on a  $10 \times 10$  grid\_trap environment. The final column shows the result obtained when combining all feedback modalities.. (a) Joint visual encoding of mean and variance. (b) Separate visual encoding of mean and variance for the same data. The rightmost column shows the result obtained when combining all feedback modalities.

## E Additional In-Distribution Results

We report performance results for all tested feedback budgets in Table 3, Table 4, Table 5, Table 7, Table 6, and Table 8.

Table 3: Full results for Grid Cliff (normalized discounted value, higher is better)

Budget (P,D,R,S)	Singles				Pairs						All	
	PDRS	PD <sub>RS</sub>	PD <sub>RS</sub>	PD <sub>RS</sub>	PDRS	PD <sub>RS</sub>						
(64, 1, 32, 128)	20.4	<b>62.6</b>	19.9	8.4	16.3	27.6	38.1	32.8	56.1	29.8	51.5	
(64, 1, 32, 256)	20.4	62.6	19.9	37.4	16.3	27.6	60.3	32.8	72.2	63.4	<b>77.8</b>	
(64, 1, 64, 128)	20.4	62.6	41.3	8.4	16.3	49.5	38.1	41.8	56.1	48.6	<b>64.7</b>	
(64, 1, 64, 256)	20.4	62.6	41.3	37.4	16.3	49.5	60.3	41.8	72.2	72.8	<b>90.8</b>	
(64, 1, 128, 128)	20.4	62.6	75.0	8.4	16.3	73.3	38.1	63.6	56.1	59.6	<b>86.6</b>	
(64, 1, 128, 256)	20.4	62.6	75.0	37.4	16.3	73.3	60.3	63.6	72.2	85.6	<b>91.0</b>	
(64, 2, 32, 128)	20.4	32.0	19.9	8.4	3.6	27.6	38.1	21.7	<b>52.4</b>	29.8	39.7	
(64, 2, 32, 256)	20.4	32.0	19.9	37.4	3.6	27.6	60.3	21.7	72.2	63.4	<b>82.3</b>	
(64, 2, 64, 128)	20.4	32.0	41.3	8.4	3.6	49.5	38.1	37.6	<b>52.4</b>	48.6	47.1	
(64, 2, 64, 256)	20.4	32.0	41.3	37.4	3.6	49.5	60.3	37.6	72.2	72.8	<b>86.6</b>	
(64, 2, 128, 128)	20.4	32.0	75.0	8.4	3.6	73.3	38.1	73.6	52.4	59.6	<b>82.2</b>	
(64, 2, 128, 256)	20.4	32.0	75.0	37.4	3.6	73.3	60.3	73.6	72.2	85.6	<b>95.5</b>	
(128, 1, 32, 128)	29.7	<b>62.6</b>	19.9	8.4	29.7	38.5	38.5	32.8	56.1	29.8	51.6	
(128, 1, 32, 256)	29.7	62.6	19.9	37.4	29.7	38.5	60.3	32.8	<b>72.2</b>	63.4	69.0	
(128, 1, 64, 128)	29.7	<b>62.6</b>	41.3	8.4	29.7	47.2	38.5	41.8	56.1	48.6	56.0	
(128, 1, 64, 256)	29.7	62.6	41.3	37.4	29.7	47.2	60.3	41.8	72.2	72.8	<b>73.4</b>	
(128, 1, 128, 128)	29.7	62.6	<b>75.0</b>	8.4	29.7	56.0	38.5	63.6	56.1	59.6	55.9	
(128, 1, 128, 256)	29.7	62.6	75.0	37.4	29.7	56.0	60.3	63.6	72.2	<b>85.6</b>	82.2	
(128, 2, 32, 128)	29.7	32.0	19.9	8.4	29.6	38.5	38.5	21.7	<b>52.4</b>	29.8	42.9	
(128, 2, 32, 256)	29.7	32.0	19.9	37.4	29.6	38.5	60.3	21.7	<b>72.2</b>	63.4	69.0	
(128, 2, 64, 128)	29.7	32.0	41.3	8.4	29.6	47.2	38.5	37.6	52.4	48.6	<b>56.0</b>	
(128, 2, 64, 256)	29.7	32.0	41.3	37.4	29.6	47.2	60.3	37.6	72.2	72.8	<b>77.9</b>	
(128, 2, 128, 128)	29.7	32.0	<b>75.0</b>	8.4	29.6	56.0	38.5	73.6	52.4	59.6	56.0	
(128, 2, 128, 256)	29.7	32.0	75.0	37.4	29.6	56.0	60.3	73.6	72.2	85.6	<b>86.7</b>	
(256, 1, 32, 128)	60.5	62.6	19.9	8.4	64.9	<b>69.3</b>	60.4	32.8	56.1	29.8	69.2	
(256, 1, 32, 256)	60.5	62.6	19.9	37.4	64.9	69.3	73.6	32.8	72.2	63.4	<b>82.3</b>	
(256, 1, 64, 128)	60.5	62.6	41.3	8.4	64.9	69.3	60.4	41.8	56.1	48.6	<b>73.6</b>	
(256, 1, 64, 256)	60.5	62.6	41.3	37.4	64.9	69.3	73.6	41.8	72.2	72.8	<b>86.7</b>	
(256, 1, 128, 128)	60.5	62.6	75.0	8.4	64.9	78.1	60.4	63.6	56.1	59.6	<b>86.8</b>	
(256, 1, 128, 256)	60.5	62.6	75.0	37.4	64.9	78.1	73.6	63.6	72.2	<b>85.6</b>	82.3	
(256, 2, 32, 128)	60.5	32.0	19.9	8.4	60.5	<b>69.3</b>	60.4	21.7	52.4	29.8	<b>69.3</b>	
(256, 2, 32, 256)	60.5	32.0	19.9	37.4	60.5	69.3	<b>73.6</b>	21.7	72.2	63.4	<b>73.6</b>	
(256, 2, 64, 128)	60.5	32.0	41.3	8.4	60.5	69.3	60.4	37.6	52.4	48.6	<b>78.1</b>	
(256, 2, 64, 256)	60.5	32.0	41.3	37.4	60.5	69.3	73.6	37.6	72.2	72.8	<b>82.5</b>	
(256, 2, 128, 128)	60.5	32.0	75.0	8.4	60.5	<b>78.1</b>	60.4	73.6	52.4	59.6	<b>78.1</b>	
(256, 2, 128, 256)	60.5	32.0	75.0	37.4	60.5	78.1	73.6	73.6	72.2	<b>85.6</b>	82.5	

Table 4: Full results for Grid Sparse (normalized discounted value, higher is better)

Budget (P,D,R,S)	Singles				Pairs						All PDRS
	PDRS	FDRS	PDRS	PDRS	PDRS	PDRS	PDRS	PDRS	PDRS	PDRS	
(64, 1, 32, 128)	4.9	65.0	20.2	25.0	-0.1	4.9	9.9	35.0	<b>80.0</b>	40.0	30.0
(64, 1, 32, 256)	4.9	65.0	20.2	35.0	-0.1	4.9	45.0	35.0	<b>75.0</b>	65.0	65.0
(64, 1, 64, 128)	4.9	65.0	35.0	25.0	-0.1	20.0	9.9	35.0	<b>80.0</b>	60.0	45.0
(64, 1, 64, 256)	4.9	65.0	35.0	35.0	-0.1	20.0	45.0	35.0	<b>75.0</b>	65.0	70.0
(64, 1, 128, 128)	4.9	65.0	75.0	25.0	-0.1	30.0	9.9	50.0	<b>80.0</b>	<b>80.0</b>	55.0
(64, 1, 128, 256)	4.9	65.0	75.0	35.0	-0.1	30.0	45.0	50.0	75.0	<b>85.0</b>	<b>85.0</b>
(64, 2, 32, 128)	4.9	45.5	20.2	25.0	-0.1	4.9	9.9	9.9	<b>70.2</b>	40.0	25.0
(64, 2, 32, 256)	4.9	45.5	20.2	35.0	-0.1	4.9	45.0	9.9	<b>85.0</b>	65.0	60.0
(64, 2, 64, 128)	4.9	45.5	35.0	25.0	-0.1	20.0	9.9	30.5	<b>70.2</b>	60.0	40.0
(64, 2, 64, 256)	4.9	45.5	35.0	35.0	-0.1	20.0	45.0	30.5	<b>85.0</b>	65.0	75.0
(64, 2, 128, 128)	4.9	45.5	75.0	25.0	-0.1	30.0	9.9	45.2	70.2	<b>80.0</b>	55.0
(64, 2, 128, 256)	4.9	45.5	75.0	35.0	-0.1	30.0	45.0	45.2	<b>85.0</b>	<b>85.0</b>	80.0
(128, 1, 32, 128)	15.0	65.0	20.2	25.0	15.0	30.0	35.0	35.0	<b>80.0</b>	40.0	40.0
(128, 1, 32, 256)	15.0	65.0	20.2	35.0	15.0	30.0	50.0	35.0	<b>75.0</b>	65.0	60.0
(128, 1, 64, 128)	15.0	65.0	35.0	25.0	15.0	35.0	35.0	35.0	<b>80.0</b>	60.0	40.0
(128, 1, 64, 256)	15.0	65.0	35.0	35.0	15.0	35.0	50.0	35.0	<b>75.0</b>	65.0	60.0
(128, 1, 128, 128)	15.0	65.0	75.0	25.0	15.0	45.0	35.0	50.0	<b>80.0</b>	<b>80.0</b>	60.0
(128, 1, 128, 256)	15.0	65.0	75.0	35.0	15.0	45.0	50.0	50.0	75.0	<b>85.0</b>	70.0
(128, 2, 32, 128)	15.0	45.5	20.2	25.0	9.9	30.0	35.0	9.9	<b>70.2</b>	40.0	35.0
(128, 2, 32, 256)	15.0	45.5	20.2	35.0	9.9	30.0	50.0	9.9	<b>85.0</b>	65.0	55.0
(128, 2, 64, 128)	15.0	45.5	35.0	25.0	9.9	35.0	35.0	30.5	<b>70.2</b>	60.0	40.0
(128, 2, 64, 256)	15.0	45.5	35.0	35.0	9.9	35.0	50.0	30.5	<b>85.0</b>	65.0	60.0
(128, 2, 128, 128)	15.0	45.5	75.0	25.0	9.9	45.0	35.0	45.2	70.2	<b>80.0</b>	60.0
(128, 2, 128, 256)	15.0	45.5	75.0	35.0	9.9	45.0	50.0	45.2	<b>85.0</b>	<b>85.0</b>	75.0
(256, 1, 32, 128)	40.0	65.0	20.2	25.0	35.0	45.0	40.0	35.0	<b>80.0</b>	40.0	60.0
(256, 1, 32, 256)	40.0	65.0	20.2	35.0	35.0	45.0	60.0	35.0	<b>75.0</b>	65.0	<b>75.0</b>
(256, 1, 64, 128)	40.0	65.0	35.0	25.0	35.0	47.3	40.0	35.0	<b>80.0</b>	60.0	65.0
(256, 1, 64, 256)	40.0	65.0	35.0	35.0	35.0	47.3	60.0	35.0	<b>75.0</b>	65.0	70.0
(256, 1, 128, 128)	40.0	65.0	75.0	25.0	35.0	50.0	40.0	50.0	<b>80.0</b>	<b>80.0</b>	70.0
(256, 1, 128, 256)	40.0	65.0	75.0	35.0	35.0	50.0	60.0	50.0	75.0	<b>85.0</b>	75.0
(256, 2, 32, 128)	40.0	45.5	20.2	25.0	40.0	45.0	40.0	9.9	<b>70.2</b>	40.0	60.0
(256, 2, 32, 256)	40.0	45.5	20.2	35.0	40.0	45.0	60.0	9.9	<b>85.0</b>	65.0	65.0
(256, 2, 64, 128)	40.0	45.5	35.0	25.0	40.0	47.3	40.0	30.5	<b>70.2</b>	60.0	60.0
(256, 2, 64, 256)	40.0	45.5	35.0	35.0	40.0	47.3	60.0	30.5	<b>85.0</b>	65.0	70.0
(256, 2, 128, 128)	40.0	45.5	75.0	25.0	40.0	50.0	40.0	45.2	70.2	<b>80.0</b>	70.0
(256, 2, 128, 256)	40.0	45.5	75.0	35.0	40.0	50.0	60.0	45.2	<b>85.0</b>	<b>85.0</b>	80.0

Table 5: Full results for Grid Trap (normalized discounted value, higher is better)

Budget (P,D,R,S)	Singles				Pairs						All	
	PDRS	FDRS	PDRS	PDRS	PDRS	PDRS	PDRS	PDRS	PDRS	PDRS	PDRS	PDRS
(64, 1, 32, 128)	49.7	15.6	55.3	-15.2	47.1	59.2	48.9	62.3	<b>72.9</b>	29.1	59.9	
(64, 1, 32, 256)	49.7	15.6	55.3	56.1	47.1	59.2	64.1	62.3	<b>69.6</b>	67.6	64.9	
(64, 1, 64, 128)	49.7	15.6	60.5	-15.2	47.1	<b>74.2</b>	48.9	58.3	72.9	69.0	67.1	
(64, 1, 64, 256)	49.7	15.6	60.5	56.1	47.1	74.2	64.1	58.3	69.6	76.2	<b>83.1</b>	
(64, 1, 128, 128)	49.7	15.6	<b>91.9</b>	-15.2	47.1	81.1	48.9	79.1	72.9	78.2	82.3	
(64, 1, 128, 256)	49.7	15.6	<b>91.9</b>	56.1	47.1	81.1	64.1	79.1	69.6	82.5	89.2	
(64, 2, 32, 128)	49.7	12.6	55.3	-15.2	46.1	59.2	48.9	0.9	51.4	29.1	<b>62.2</b>	
(64, 2, 32, 256)	49.7	12.6	55.3	56.1	46.1	59.2	64.1	0.9	<b>73.6</b>	67.6	66.8	
(64, 2, 64, 128)	49.7	12.6	60.5	-15.2	46.1	<b>74.2</b>	48.9	38.7	51.4	69.0	64.1	
(64, 2, 64, 256)	49.7	12.6	60.5	56.1	46.1	74.2	64.1	38.7	73.6	76.2	<b>77.6</b>	
(64, 2, 128, 128)	49.7	12.6	<b>91.9</b>	-15.2	46.1	81.1	48.9	72.2	51.4	78.2	72.2	
(64, 2, 128, 256)	49.7	12.6	<b>91.9</b>	56.1	46.1	81.1	64.1	72.2	73.6	82.5	86.5	
(128, 1, 32, 128)	72.2	15.6	55.3	-15.2	59.5	<b>78.4</b>	62.2	62.3	72.9	29.1	67.6	
(128, 1, 32, 256)	72.2	15.6	55.3	56.1	59.5	78.4	78.4	62.3	69.6	67.6	<b>86.7</b>	
(128, 1, 64, 128)	72.2	15.6	60.5	-15.2	59.5	<b>81.1</b>	62.2	58.3	72.9	69.0	77.6	
(128, 1, 64, 256)	72.2	15.6	60.5	56.1	59.5	81.1	78.4	58.3	69.6	76.2	<b>86.5</b>	
(128, 1, 128, 128)	72.2	15.6	<b>91.9</b>	-15.2	59.5	83.8	62.2	79.1	72.9	78.2	81.1	
(128, 1, 128, 256)	72.2	15.6	<b>91.9</b>	56.1	59.5	83.8	78.4	79.1	69.6	82.5	86.5	
(128, 2, 32, 128)	72.2	12.6	55.3	-15.2	46.1	<b>78.4</b>	62.2	0.9	51.4	29.1	67.6	
(128, 2, 32, 256)	72.2	12.6	55.3	56.1	46.1	78.4	78.4	0.9	73.6	67.6	<b>83.8</b>	
(128, 2, 64, 128)	72.2	12.6	60.5	-15.2	46.1	<b>81.1</b>	62.2	38.7	51.4	69.0	73.0	
(128, 2, 64, 256)	72.2	12.6	60.5	56.1	46.1	81.1	78.4	38.7	73.6	76.2	<b>86.5</b>	
(128, 2, 128, 128)	72.2	12.6	<b>91.9</b>	-15.2	46.1	83.8	62.2	72.2	51.4	78.2	83.8	
(128, 2, 128, 256)	72.2	12.6	<b>91.9</b>	56.1	46.1	83.8	78.4	72.2	73.6	82.5	86.5	
(256, 1, 32, 128)	75.7	15.6	55.3	-15.2	70.3	<b>78.4</b>	75.7	62.3	72.9	29.1	73.0	
(256, 1, 32, 256)	75.7	15.6	55.3	56.1	70.3	78.4	75.9	62.3	69.6	67.6	<b>81.1</b>	
(256, 1, 64, 128)	75.7	15.6	60.5	-15.2	70.3	<b>81.1</b>	75.7	58.3	72.9	69.0	78.4	
(256, 1, 64, 256)	75.7	15.6	60.5	56.1	70.3	<b>81.1</b>	75.9	58.3	69.6	76.2	<b>81.1</b>	
(256, 1, 128, 128)	75.7	15.6	<b>91.9</b>	-15.2	70.3	81.1	75.7	79.1	72.9	78.2	83.8	
(256, 1, 128, 256)	75.7	15.6	<b>91.9</b>	56.1	70.3	81.1	75.9	79.1	69.6	82.5	86.5	
(256, 2, 32, 128)	75.7	12.6	55.3	-15.2	67.6	<b>78.4</b>	75.7	0.9	51.4	29.1	73.0	
(256, 2, 32, 256)	75.7	12.6	55.3	56.1	67.6	78.4	75.9	0.9	73.6	67.6	<b>81.1</b>	
(256, 2, 64, 128)	75.7	12.6	60.5	-15.2	67.6	<b>81.1</b>	75.7	38.7	51.4	69.0	73.0	
(256, 2, 64, 256)	75.7	12.6	60.5	56.1	67.6	<b>81.1</b>	75.9	38.7	73.6	76.2	78.4	
(256, 2, 128, 128)	75.7	12.6	<b>91.9</b>	-15.2	67.6	81.1	75.7	72.2	51.4	78.2	83.8	
(256, 2, 128, 256)	75.7	12.6	<b>91.9</b>	56.1	67.6	81.1	75.9	72.2	73.6	82.5	89.3	

Table 6: Full results for Acrobot (v1) (normalized return, higher is better)

Budget (P,D,R,S)	Singles				Pairs						All	
	PDRS	PD <sub>RS</sub>	PD <sub>RS</sub>	PD <sub>RS</sub>	PDRS	PD <sub>RS</sub>						
(256, 1, 32, 64)	53.3	96.6	97.9	87.6	95.5	74.8	83.0	98.1	<b>98.8</b>	98.3	96.4	
(256, 1, 32, 128)	53.3	96.6	97.9	<b>99.1</b>	95.5	74.8	93.2	98.1	98.8	98.5	98.7	
(256, 1, 64, 64)	53.3	96.6	98.2	87.6	95.5	76.6	83.0	<b>99.0</b>	98.8	97.4	98.1	
(256, 1, 64, 128)	53.3	96.6	98.2	99.1	95.5	76.6	93.2	99.0	98.8	<b>99.3</b>	98.6	
(256, 1, 128, 64)	53.3	96.6	98.6	87.6	95.5	76.1	83.0	98.7	98.8	98.8	<b>98.9</b>	
(256, 1, 128, 128)	53.3	96.6	98.6	99.1	95.5	76.1	93.2	98.7	98.8	<b>99.2</b>	98.5	
(256, 2, 32, 64)	53.3	98.2	97.9	87.6	98.0	74.8	83.0	97.9	<b>98.7</b>	98.3	98.7	
(256, 2, 32, 128)	53.3	98.2	97.9	99.1	98.0	74.8	93.2	97.9	<b>99.1</b>	98.5	98.5	
(256, 2, 64, 64)	53.3	98.2	98.2	87.6	98.0	76.6	83.0	<b>98.9</b>	98.7	97.4	98.3	
(256, 2, 64, 128)	53.3	98.2	98.2	99.1	98.0	76.6	93.2	98.9	99.1	<b>99.3</b>	98.6	
(256, 2, 128, 64)	53.3	98.2	98.6	87.6	98.0	76.1	83.0	98.8	98.7	<b>98.8</b>	98.0	
(256, 2, 128, 128)	53.3	98.2	98.6	99.1	98.0	76.1	93.2	98.8	99.1	<b>99.2</b>	99.1	
(256, 4, 32, 64)	53.3	<b>99.5</b>	97.9	87.6	96.3	74.8	83.0	98.0	97.3	98.3	98.4	
(256, 4, 32, 128)	53.3	<b>99.5</b>	97.9	99.1	96.3	74.8	93.2	98.0	98.9	98.5	99.1	
(256, 4, 64, 64)	53.3	<b>99.5</b>	98.2	87.6	96.3	76.6	83.0	99.4	97.3	97.4	98.9	
(256, 4, 64, 128)	53.3	<b>99.5</b>	98.2	99.1	96.3	76.6	93.2	99.4	98.9	99.3	98.6	
(256, 4, 128, 64)	53.3	<b>99.5</b>	98.6	87.6	96.3	76.1	83.0	99.0	97.3	98.8	98.9	
(256, 4, 128, 128)	53.3	<b>99.5</b>	98.6	99.1	96.3	76.1	93.2	99.0	98.9	99.2	98.8	
(256, 4, 256, 64)	53.3	<b>99.5</b>	97.9	87.6	96.3	96.3	83.0	99.3	97.3	99.0	98.8	
(256, 4, 256, 128)	53.3	<b>99.5</b>	97.9	99.1	96.3	96.3	93.2	99.3	98.9	99.2	99.0	
(256, 4, 512, 64)	53.3	<b>99.5</b>	73.4	87.6	96.3	70.7	83.0	99.2	97.3	<b>98.1</b>	99.1	
(256, 4, 512, 128)	53.3	<b>99.5</b>	73.4	99.1	96.3	70.7	93.2	99.2	98.9	99.5	99.4	
(512, 1, 32, 64)	53.3	96.6	97.9	87.6	94.3	60.6	96.6	98.1	<b>98.8</b>	98.3	97.6	
(512, 1, 32, 128)	53.3	96.6	97.9	<b>99.1</b>	94.3	60.6	79.8	98.1	98.8	98.5	98.6	
(512, 1, 64, 64)	53.3	96.6	98.2	87.6	94.3	84.8	96.6	<b>99.0</b>	98.8	97.4	98.5	
(512, 1, 64, 128)	53.3	96.6	98.2	99.1	94.3	84.8	79.8	99.0	98.8	<b>99.3</b>	98.4	
(512, 1, 128, 64)	53.3	96.6	98.6	87.6	94.3	78.4	96.6	98.7	98.8	<b>98.8</b>	98.6	
(512, 1, 128, 128)	53.3	96.6	98.6	99.1	94.3	78.4	79.8	98.7	98.8	<b>99.2</b>	98.8	
(512, 2, 32, 64)	53.3	98.2	97.9	87.6	97.4	60.6	96.6	97.9	<b>98.7</b>	98.3	98.4	
(512, 2, 32, 128)	53.3	98.2	97.9	99.1	97.4	60.6	79.8	97.9	<b>99.1</b>	98.5	98.2	
(512, 2, 64, 64)	53.3	98.2	98.2	87.6	97.4	84.8	96.6	<b>98.9</b>	98.7	97.4	98.6	
(512, 2, 64, 128)	53.3	98.2	98.2	99.1	97.4	84.8	79.8	98.9	99.1	<b>99.3</b>	98.4	
(512, 2, 128, 64)	53.3	98.2	98.6	87.6	97.4	78.4	96.6	98.8	98.7	98.8	<b>98.9</b>	
(512, 2, 128, 128)	53.3	98.2	98.6	99.1	97.4	78.4	79.8	98.8	99.1	<b>99.2</b>	99.1	
(512, 4, 32, 64)	53.3	<b>99.5</b>	97.9	87.6	98.3	60.6	96.6	98.0	97.3	98.3	99.2	
(512, 4, 32, 128)	53.3	<b>99.5</b>	97.9	99.1	98.3	60.6	79.8	98.0	98.9	98.5	99.0	
(512, 4, 64, 64)	53.3	<b>99.5</b>	98.2	87.6	98.3	84.8	96.6	99.4	97.3	97.4	99.2	
(512, 4, 64, 128)	53.3	<b>99.5</b>	98.2	99.1	98.3	84.8	79.8	99.4	98.9	99.3	99.1	
(512, 4, 128, 64)	53.3	<b>99.5</b>	98.6	87.6	98.3	78.4	96.6	99.0	97.3	98.8	98.8	
(512, 4, 128, 128)	53.3	<b>99.5</b>	98.6	99.1	98.3	78.4	79.8	99.0	98.9	99.2	99.2	
(512, 4, 256, 64)	53.3	<b>99.5</b>	97.9	87.6	98.3	88.8	96.6	99.3	97.3	99.0	99.0	
(512, 4, 256, 128)	53.3	<b>99.5</b>	97.9	99.1	98.3	88.8	79.8	99.3	98.9	99.2	99.2	
(512, 4, 512, 64)	53.3	<b>99.5</b>	73.4	87.6	98.3	97.3	96.6	99.2	97.3	98.1	99.1	
(512, 4, 512, 128)	53.3	<b>99.5</b>	73.4	99.1	98.3	97.3	79.8	99.2	98.9	99.5	99.1	

Table 7: Full results for CartPole (v1) (normalized return, higher is better)

Budget (P,D,R,S)	Singles				Pairs						All	
	PDRS	PDRS	PDRS	PDRS	PDRS	PDRS	PDRS	PDRS	PDRS	PDRS	PDRS	PDRS
(256, 1, 32, 64)	64.7	24.2	<b>81.4</b>	-1.3	50.8	71.5	51.1	32.7	-1.0	33.3	37.3	
(256, 1, 32, 128)	64.7	24.2	<b>81.4</b>	1.0	50.8	71.5	44.1	32.7	-1.4	27.4	26.9	
(256, 1, 64, 64)	64.7	24.2	78.5	-1.3	50.8	<b>82.3</b>	51.1	45.0	-1.0	51.8	32.9	
(256, 1, 64, 128)	64.7	24.2	78.5	1.0	50.8	<b>82.3</b>	44.1	45.0	-1.4	58.7	27.4	
(256, 1, 128, 64)	64.7	24.2	73.8	-1.3	50.8	<b>92.5</b>	51.1	59.3	-1.0	74.7	62.3	
(256, 1, 128, 128)	64.7	24.2	73.8	1.0	50.8	<b>92.5</b>	44.1	59.3	-1.4	57.4	46.2	
(256, 2, 32, 64)	64.7	38.4	<b>81.4</b>	-1.3	62.9	71.5	51.1	38.1	4.8	33.3	48.4	
(256, 2, 32, 128)	64.7	38.4	<b>81.4</b>	1.0	62.9	71.5	44.1	38.1	-1.3	27.4	24.9	
(256, 2, 64, 64)	64.7	38.4	78.5	-1.3	62.9	<b>82.3</b>	51.1	37.2	4.8	51.8	42.5	
(256, 2, 64, 128)	64.7	38.4	78.5	1.0	62.9	<b>82.3</b>	44.1	37.2	-1.3	58.7	34.5	
(256, 2, 128, 64)	64.7	38.4	73.8	-1.3	62.9	<b>92.5</b>	51.1	62.3	4.8	74.7	57.2	
(256, 2, 128, 128)	64.7	38.4	73.8	1.0	62.9	<b>92.5</b>	44.1	62.3	-1.3	57.4	37.7	
(256, 4, 32, 64)	64.7	26.5	<b>81.4</b>	-1.3	66.1	71.5	51.1	40.8	12.2	33.3	29.6	
(256, 4, 32, 128)	64.7	26.5	<b>81.4</b>	1.0	66.1	71.5	44.1	40.8	1.7	27.4	23.1	
(256, 4, 64, 64)	64.7	26.5	78.5	-1.3	66.1	<b>82.3</b>	51.1	46.2	12.2	51.8	41.6	
(256, 4, 64, 128)	64.7	26.5	78.5	1.0	66.1	<b>82.3</b>	44.1	46.2	1.7	58.7	51.5	
(256, 4, 128, 64)	64.7	26.5	73.8	-1.3	66.1	<b>92.5</b>	51.1	72.7	12.2	74.7	61.7	
(256, 4, 128, 128)	64.7	26.5	73.8	1.0	66.1	<b>92.5</b>	44.1	72.7	1.7	57.4	50.9	
(256, 4, 256, 64)	64.7	26.5	69.8	-1.3	66.1	<b>97.7</b>	51.1	62.5	12.2	93.8	87.5	
(256, 4, 256, 128)	64.7	26.5	69.8	1.0	66.1	<b>97.7</b>	44.1	62.5	1.7	70.5	72.3	
(256, 4, 512, 64)	64.7	26.5	<b>96.4</b>	-1.3	66.1	96.2	51.1	87.7	12.2	93.4	81.9	
(256, 4, 512, 128)	64.7	26.5	96.4	1.0	66.1	96.2	44.1	87.7	1.7	<b>98.4</b>	86.7	
(512, 1, 32, 64)	67.1	24.2	81.4	-1.3	66.8	<b>94.7</b>	43.7	32.7	-1.0	33.3	43.3	
(512, 1, 32, 128)	67.1	24.2	81.4	1.0	66.8	<b>94.7</b>	50.4	32.7	-1.4	27.4	34.0	
(512, 1, 64, 64)	67.1	24.2	78.5	-1.3	66.8	<b>88.7</b>	43.7	45.0	-1.0	51.8	50.0	
(512, 1, 64, 128)	67.1	24.2	78.5	1.0	66.8	<b>88.7</b>	50.4	45.0	-1.4	58.7	31.1	
(512, 1, 128, 64)	67.1	24.2	73.8	-1.3	66.8	<b>99.9</b>	43.7	59.3	-1.0	74.7	53.7	
(512, 1, 128, 128)	67.1	24.2	73.8	1.0	66.8	<b>99.9</b>	50.4	59.3	-1.4	57.4	42.8	
(512, 2, 32, 64)	67.1	38.4	81.4	-1.3	83.4	<b>94.7</b>	43.7	38.1	4.8	33.3	44.6	
(512, 2, 32, 128)	67.1	38.4	81.4	1.0	83.4	<b>94.7</b>	50.4	38.1	-1.3	27.4	41.2	
(512, 2, 64, 64)	67.1	38.4	78.5	-1.3	83.4	<b>88.7</b>	43.7	37.2	4.8	51.8	55.8	
(512, 2, 64, 128)	67.1	38.4	78.5	1.0	83.4	<b>88.7</b>	50.4	37.2	-1.3	58.7	42.5	
(512, 2, 128, 64)	67.1	38.4	73.8	-1.3	83.4	<b>99.9</b>	43.7	62.3	4.8	74.7	67.6	
(512, 2, 128, 128)	67.1	38.4	73.8	1.0	83.4	<b>99.9</b>	50.4	62.3	-1.3	57.4	48.8	
(512, 4, 32, 64)	67.1	26.5	81.4	-1.3	78.6	<b>94.7</b>	43.7	40.8	12.2	33.3	41.3	
(512, 4, 32, 128)	67.1	26.5	81.4	1.0	78.6	<b>94.7</b>	50.4	40.8	1.7	27.4	29.6	
(512, 4, 64, 64)	67.1	26.5	78.5	-1.3	78.6	<b>88.7</b>	43.7	46.2	12.2	51.8	47.7	
(512, 4, 64, 128)	67.1	26.5	78.5	1.0	78.6	<b>88.7</b>	50.4	46.2	1.7	58.7	30.5	
(512, 4, 128, 64)	67.1	26.5	73.8	-1.3	78.6	<b>99.9</b>	43.7	72.7	12.2	74.7	48.4	
(512, 4, 128, 128)	67.1	26.5	73.8	1.0	78.6	<b>99.9</b>	50.4	72.7	1.7	57.4	47.6	
(512, 4, 256, 64)	67.1	26.5	69.8	-1.3	78.6	<b>100.0</b>	43.7	62.5	12.2	93.8	88.1	
(512, 4, 256, 128)	67.1	26.5	69.8	1.0	78.6	<b>100.0</b>	50.4	62.5	1.7	70.5	52.0	
(512, 4, 512, 64)	67.1	26.5	96.4	-1.3	78.6	<b>98.5</b>	43.7	87.7	12.2	93.4	85.5	
(512, 4, 512, 128)	67.1	26.5	96.4	1.0	78.6	<b>98.5</b>	50.4	87.7	1.7	98.4	85.8	

Table 8: Full results for LunarLander-v3 (normalized return, higher is better)

Budget (P,D,R,S)	Singles				Pairs						All	
	PDRS	PDRS	PDRS	PDRS	PDRS	PDRS	PDRS	PDRS	PDRS	PDRS	PDRS	PDRS
(512, 1, 512, 128)	-15.8	-0.2	<b>23.7</b>	-30.3	-3.7	11.7	-15.9	-38.4	-59.1	-11.0	-2.1	
(512, 1, 512, 256)	-15.8	-0.2	<b>23.7</b>	-22.2	-3.7	11.7	1.4	-38.4	-10.4	15.1	2.0	
(512, 1, 1024, 128)	-15.8	-0.2	3.6	-30.3	-3.7	-0.2	-15.9	-13.0	-59.1	<b>11.6</b>	2.9	
(512, 1, 1024, 256)	-15.8	-0.2	3.6	-22.2	-3.7	-0.2	1.4	-13.0	-10.4	<b>17.6</b>	11.2	
(512, 2, 512, 128)	-15.8	<b>108.9</b>	23.7	-30.3	-12.8	11.7	-15.9	-16.2	-25.3	-11.0	-7.5	
(512, 2, 512, 256)	-15.8	<b>108.9</b>	23.7	-22.2	-12.8	11.7	1.4	-16.2	-13.9	15.1	17.5	
(512, 2, 1024, 128)	-15.8	<b>108.9</b>	3.6	-30.3	-12.8	-0.2	-15.9	-1.1	-25.3	11.6	10.4	
(512, 2, 1024, 256)	-15.8	<b>108.9</b>	3.6	-22.2	-12.8	-0.2	1.4	-1.1	-13.9	17.6	6.5	
(512, 4, 512, 128)	-15.8	<b>113.7</b>	23.7	-30.3	-29.0	11.7	-15.9	8.2	-34.5	-11.0	12.2	
(512, 4, 512, 256)	-15.8	<b>113.7</b>	23.7	-22.2	-29.0	11.7	1.4	8.2	5.0	15.1	20.2	
(512, 4, 1024, 128)	-15.8	<b>113.7</b>	3.6	-30.3	-29.0	-0.2	-15.9	8.0	-34.5	11.6	7.8	
(512, 4, 1024, 256)	-15.8	<b>113.7</b>	3.6	-22.2	-29.0	-0.2	1.4	8.0	5.0	17.6	24.7	
(512, 32, 512, 128)	-15.8	<b>115.6</b>	23.7	-30.3	39.3	11.7	-15.9	42.7	39.3	-11.0	59.7	
(512, 32, 512, 256)	-15.8	<b>115.6</b>	23.7	-22.2	39.3	11.7	1.4	42.7	55.7	15.1	63.4	
(512, 32, 1024, 128)	-15.8	<b>115.6</b>	3.6	-30.3	39.3	-0.2	-15.9	38.3	39.3	11.6	71.3	
(512, 32, 1024, 256)	-15.8	<b>115.6</b>	3.6	-22.2	39.3	-0.2	1.4	38.3	55.7	17.6	73.9	
(1024, 1, 512, 128)	-3.8	-0.2	<b>23.7</b>	-30.3	14.3	-7.1	-2.6	-38.4	-59.1	-11.0	11.8	
(1024, 1, 512, 256)	-3.8	-0.2	<b>23.7</b>	-22.2	14.3	-7.1	1.2	-38.4	-10.4	15.1	7.9	
(1024, 1, 1024, 128)	-3.8	-0.2	3.6	-30.3	14.3	4.0	-2.6	-13.0	-59.1	11.6	<b>16.3</b>	
(1024, 1, 1024, 256)	-3.8	-0.2	3.6	-22.2	14.3	4.0	1.2	-13.0	-10.4	<b>17.6</b>	8.9	
(1024, 2, 512, 128)	-3.8	<b>108.9</b>	23.7	-30.3	4.5	-7.1	-2.6	-16.2	-25.3	-11.0	-1.2	
(1024, 2, 512, 256)	-3.8	<b>108.9</b>	23.7	-22.2	4.5	-7.1	1.2	-16.2	-13.9	15.1	20.5	
(1024, 2, 1024, 128)	-3.8	<b>108.9</b>	3.6	-30.3	4.5	4.0	-2.6	-1.1	-25.3	11.6	8.5	
(1024, 2, 1024, 256)	-3.8	<b>108.9</b>	3.6	-22.2	4.5	4.0	1.2	-1.1	-13.9	17.6	-0.3	
(1024, 4, 512, 128)	-3.8	<b>113.7</b>	23.7	-30.3	11.2	-7.1	-2.6	8.2	-34.5	-11.0	8.0	
(1024, 4, 512, 256)	-3.8	<b>113.7</b>	23.7	-22.2	11.2	-7.1	1.2	8.2	5.0	15.1	18.5	
(1024, 4, 1024, 128)	-3.8	<b>113.7</b>	3.6	-30.3	11.2	4.0	-2.6	8.0	-34.5	11.6	22.6	
(1024, 4, 1024, 256)	-3.8	<b>113.7</b>	3.6	-22.2	11.2	4.0	1.2	8.0	5.0	17.6	23.0	
(1024, 32, 512, 128)	-3.8	<b>115.6</b>	23.7	-30.3	30.0	-7.1	-2.6	42.7	39.3	-11.0	71.0	
(1024, 32, 512, 256)	-3.8	<b>115.6</b>	23.7	-22.2	30.0	-7.1	1.2	42.7	55.7	15.1	77.8	
(1024, 32, 1024, 128)	-3.8	<b>115.6</b>	3.6	-30.3	30.0	4.0	-2.6	38.3	39.3	11.6	67.2	
(1024, 32, 1024, 256)	-3.8	<b>115.6</b>	3.6	-22.2	30.0	4.0	1.2	38.3	55.7	17.6	80.4	